Erasmus Mundus Master in Membrane Engineering for a Sustainable World (www.em3e.eu)

Academic year 2018-2019

Semester 4

Final Master Thesis Report

Topic

Direct Sunlight for membrane distillation based on photothermal membranes

Submitted By

SWARNA, Sutapa Roy
NANOMAT, Universidad de Zaragoza
EM3E-4SW

Supervisor

Professor Reyes Mallada

Universidad de Zaragoza

Submitted To

Professor André Ayral

Ing. Vlastimil Fila

Dra. María Pilar Pina

6.09.2019

"The EM3E4SW Master is an Education Programme supported by the European Commission, the European Membrane Society (EMS), the European Membrane House (EMH), and a large international network of industrial companies, research centres and universities"

"The EM3E4SW education programme has been founded with support from the European Commission. This publication reflects the views only of the author, and the Commission cannot be held responsible for any use which may be made of information contained therein".

Acknowledgment:

I would like to start by expressing my special and utmost gratitude to my supervisor Prof. Reyes Mallada. More than being just a teacher to me, she has been a mother figure to me who I really needed at times. She helped me in ways that I cannot even express in words. If she were not there, maybe I would not be able to even try to finish my report. She has only encouraged me and gave me strength I could not use it properly. I cannot say it enough to express how indebted I am to her. Thank you for your patience and support.

I would like to extend my gratitude to the European Institute of Membranes in Montpellier and the partner universities involved in my formation during this master: University of Montpellier II, Universite –Toulouse III Paul Sabatier, University of Chemistry and Technology of Prague, University of Zaragoza. Also, I would like to thank the European Commission for the economic support and Prof. André Ayral to give me the extension and giving me the opportunity to try at least. I also thank Karin for the support.

I would thank to my family, my friend Tasmia, Jessica, Sebastian, Jasmin to give me support and hope when I needed it the most. My psychologist Elizabeth, thank you. Thanks to all the people in the lab who helped me in every step. Thanks to everyone who helped me to live a little longer and better.

Contents

Table of Figures:

1. Introduction:

As the number of people will keep increasing in the world, the freshwater will be demanded than more than anything. Limited resource of freshwater underground, ground rivers will not be sufficient to meet the demand and urge to look for new options will be encouraged. 97.5% of water belongs to seas and only 0.79% of freshwater is recoverable from the remaining 2.5% is fresh water.[1] Membrane distillation (MD) can be appointed in desalination process to provide fresh water.

MD defined as thermal membrane process where the driving force is the transmembrane vapor pressure difference and vapor–liquid interface equilibrium is established in the pore to facilitate the vapor transfer through the membrane pores to the comparatively colder distillate side.[2][3] In order to facilitate MD operation, high membrane hydrophobicity is considered one of the primary requirements as hydrophobicity provide a barrier to liquid water passage to the permeate side but promotes vapor transport through membrane.[4] Other requirements Lawson and Lloyd (1997) are: i) Porous membrane; ii) Non-wetted membrane by process liquid; iii) No capillary condensation inside the membrane pore; iv) No alteration of the vapor/liquid equilibrium of the different components in the process liquids by the membrane; v) one side of the membrane in direct contact with the process liquid etc.[5]

Among the types of MD, there are four as follow: direct contact membrane distillation (DCMD), air gap membrane distillation (AGMD), sweeping gas membrane distillation (SGMD), vacuum membrane distillation (VMD).[1][6] Another one adds into these names nanophotonics-enabled

solar membrane distillation (NESMD), can be considered as a take on DCMD where local heating of a nanoparticle (NP)-infused membrane when it is illuminated by solar energy or photothermal energy.[7] Advantages such as MD is simple, absence of applied hydraulic pressure, achievable and inexpensive material and 100% theoretical salt rejection get weighed down by disadvantages like it consumes higher energy, has energy loss, temperature polarization, needs extra solar-thermal collector etc.[1][2][8][9]

Temperature polarization refers the situation as the temperature at the membrane surface on the feed side (T_1) may be significantly lower than the temperature of the bulk heated feed water (T_F), and when the vapor will pass down to distillate side temperature at the membrane surface on the distillate side (T_2) may be significantly higher than that of the bulk distillate (T_D).

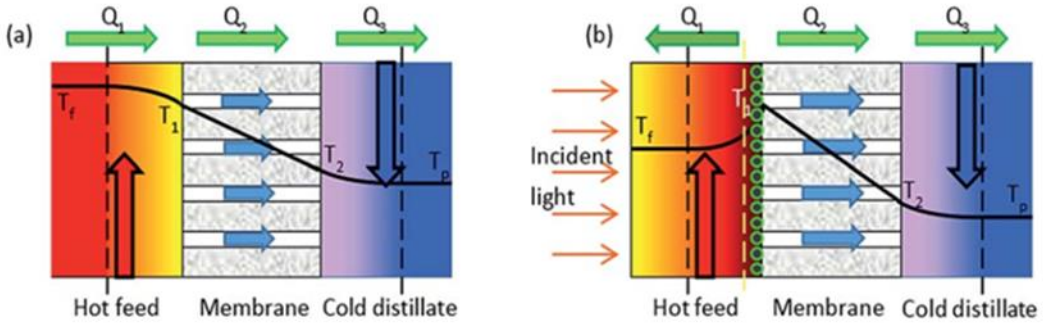

Figure 1: Presentation of (a) Conventional Membrane distillation; (b) proposed membrane distillation with nanomaterials deposited (or coating) on membrane for localized heating [4]

So, if the water is only heated locally when it is in direct contact with the one surface of the membrane, TP can be minimized to quite some extent as the temperature will not get down at the vicinity of the membrane. And to get local heating, photothermal membrane (coating or deposited nanoparticles on membrane which gets heated under visible or solar light) can be employed which provides providing the thermal driving force for the MD process.[4]

From recent past, there is a wave of appreciation for renewable energy. Among them, solar energy is considered one of the promising options as it is stated that per hour, sunlight strikes the earth surface with more energy than the summation of the energy consumed by human in a whole year. Additionally, solar energy surpassing renewable and fossil-based energy resources combined opens up a broad range application area.[10] Polytetrafluoroethylene (PTFE), polypropylene (PP)

and polyvinylidene fluoride (PVDF, good physical, chemical, and mechanical properties including lower surface energy)[6] are used for synthesizing MD membrane.[1]

Literature Review: As metallic nanoparticles act as good optical absorber attributing to the surface plasmon resonance[11], different kinds of nanoparticle varying size, shape, synthesis process, operating module and/or system have been employed to test out and evaluate the performances. Though this work incorporated nanoparticles on the membrane, there are journal papers exploring other arrangements. Local steam generation using cold bulk liquid with dispersed **i)** silica core-Au nanoshells; **ii)** water-soluble N115 carbon black (CB) nanoparticles were tried out using high intensity of sunlight (solar light focused using 26.67 cm ×26.67 cm Fresnel lens, wavelength range: 400-1300 nm) with power of 10^3 kW m^{-2} showed quite similar trend for both cases and produced 2.5 g steam was generated in 4 minutes with 24% steam generation efficiency. Increment of temperature found out to be depended on the fluid volume (increment of nanoparticles).[11] Using quite similar nanoparticles mentioned aforementioned paper[11], photothermal modified hydrophobic commercial PVDF membranes depositing **i)** SiO_2 core (120 nm) with Au nanoshells (20 nm thickness) and **ii)** unfunctionalized CB NPs on them varying coating density, were chosen as experimental membranes in direct contact solar membrane distillation system. The membrane module with an effective area of 28.3 cm^2 used a quartz window allowing irradiation of the membrane surface measured 1 sun unit (~1.367 kWm^{-2}) and the simulated sunlight is provided by six halogen tungsten lamps. The countercurrent feed and distillate flowrates were 8.5 cms^{-1} and 7.76 cms^{-1} (Reynolds numbers of 470 and 309 respectively) though peristaltic pump. Low coating density of CB gives 0.22 $gm^{-2}s^{-1}$ whereas membrane with higher coating density CB achieved 0.42 $gm^{-2}s^{-1}$ permeate flux expected due to high number of CB on the membrane with photothermal efficiency 74.6%. On the other hand, SiO_2-Au core-nanoshells gives 0.25 $gm^{-2}s^{-1}$.[8] A double layer structure (DLS) consisting thermally insulating carbon foam supporting a photothermal exfoliated graphite layer exposed under solar simulator (Xe lamp, wavelength range: 200–1500 nm) with an optical filter and copper aperture. The water was kept on the bottom and open steam generation (evaporation of vapor from top) was presented for both 1 kWm^{-2} and 10 kWm^{-2}. Evaporation rate 0.28 $gm^{-2}s^{-1}$ at 64% photothermal efficiency for 1 kWm^{-2} and approximately 3.07 $gm^{-2}s^{-1}$ at 85% thermal efficiency were reported.[12] 300 W Xe lamp with UV-vis mirror module (wavelength range:300 to 600 nm) was focused on anodized alumina membrane and also azobenzene modified (2.5 cm diameter; 4.9 cm^2 area). It shows the highest water permeation flux 0.007 $gm^{-2}s^{-1}$ for

anodized alumina membrane and even less for other two azobenzene modified membranes.[13] Flexible thin-film black gold membranes with multiscale structures of microscale funnel structures and varying metallic nanoscale gaps was studied to find the optimal taper angle with the goal to conduct efficient solar steam generation creating high surface plasmon dissipation losses for heat generation and the high light absorption in the metal structure. The system consisted floating multilayered (to reduce the optical loss by light transmission) black gold membrane peeled off by microporous substrate (3M Micropore Surgical Tape) on the surface of water under illumination source Xe arc lamp with air mass filter (wavelength range: 400-2500 nm). Evaporation rate 4.34 $gm^{-2}s^{-1}$ with thermal efficiency 57% at an incident intensity of 20 kWm^{-2} was recorded.[14] Bilayer membrane of a 25 μm electrospun photothermal nanocomposite coating of surface oxidized CB NPs embedded in polyvinyl alcohol (PVA) on top of a polydopamine layer aided commercial PVDF membrane was installed on a module under outdoor sunlight providing average solar intensity 0.7 kWm^{-2} (illumination through 3.3 ×6.8-cm quartz window). Small-scale NESMD module (8.1 cm×3.48 cm) had a flux of 0.06 g m^{-2} s^{-1} with 53.8% photothermal efficiency[7]**.** The journal paper which was followed to an extent for the module and system building used flat-sheet microporous hydrophobic PVDF membranes embedding Ag NPs (range: 25-35 nm, 15-25% loading) prepared by a nonsolvent-induced phase-inversion process was inspected for photothermal membrane distillation for seawater desalination. Effective membrane area 21.24 cm^2 was exposed under UV Hg lamp at 366 nm at 90° viewing angle and the experiment was carried under conditions as 5.5 × 10−6 m^3s^{-1} by using a peristaltic pump; vacuum pressure of 20 mbar (0.59 in Hg) and initial feed temperature of 303 K, irradiance 23 kWm^{-2} giving average transmembrane flux for pure water following 4.08 $gm^{-2}s^{-1}$, 7.52 $gm^{-2}s^{-1}$, 8.94 $gm^{-2}s^{-1}$ for 15%, 20% and 25% Ag NPs loading in the PVDF membrane respectively. The experiment was also done for 0.5 M NaCl solution to replicate condition similar to seawater to evaluate the membrane's desalination performance giving highest 7.13 $gm^{-2}s^{-1}$ transmembrane flux for 25% Ag loading membrane.[9] There was another process to synthesis aqueous based Au NPs using Chloroauric acid (HAuCl4) and Poly (acrylic acid, sodium salt) using microwave heating. Though the synthesis time was really short and convenient, the NPs size was really small and they had random clusters of NPs. As it was the motive to have a homogeneous deposition on membrane, this synthesis process was not pursued further.

In this report, hydrophilic and hydrophobic PVDF membranes are used for respective Au NPs (Au-citrate and Au-thiol) incorporation. Nanoparticles synthesis and characterization, different deposition techniques, system setup, temperature profile under different wavelength LEDs varying distance between LED and membrane, batch experiment with newly altered module and other different perspectives will be realized.

2. Objective:

- Synthesis of Au NPs and characterization
- Experimenting with different ways of deposition of NPs on membrane
    - Hydrophobic NPs on hydrophobic membrane
    - Hydrophilic NPs on hydrophilic membrane and then hydrophobizing the surface
- Set-up a membrane distillation unit correcting the previous model
- Experimental results: Temperature profiles and batch experiment

3. Experimental Procedure:

3.1. Au-citrate synthesis:

The citrate capped Au nanoparticles were synthesized via a modified version of Turkevich-Frens method described in the paper cited [15]. The procedure followed heating of 50 mL of aqueous solution (1.1 mM) of Chloroauric acid ($HAuCl_4$, 50% Au basis) at 70 ^{o}C under continuous stirring in water bath and then adding 5 mL of preheated sodium citrate aqueous solution (3.8 mM). The temperature of the mixture was maintained at 70 °C until a red-wine color appeared. 10 minutes was given for the seeds to grow and creating citrate capping around Au nanoparticles. The aqueous suspension was allowed to cool down to room temperature and then, aluminium foil covered vial was kept in the refrigerator to avoid direct light interaction.

3.2. Au-thiol synthesis:

To change the citrate capping of the previously produced Au NPs to thiol ligand in order to give the Au NPs hydrophobicity, an elaborate procedure was followed. 15 ml of freshly produced Au-citrate suspension synthesized following the procedure described in section 3.1. was taken for the ligand changing. 1-octadecanethiol (98%, 7 gm) is dissolved in hexane (95%, 30 ml) at high stirring mode. When it got fully dissolved, 15 ml of Au-citrate suspension was added to it. After

adding them together, they show two quite immiscible different layers in the vial. Upper one was a little opaque organic phase (hexane and 1-Octadecanethiol) and the bottom part was red wine color aqueous phase (Au-citrate NPs suspension). The vial was placed on a stirring plate and stirring mode was set for 45 minutes at room temperature ensuring that there was a homogeneous mixing between two layers to facilitate good contact. After 45 minutes it was noticed that still there were 2 layers but the color of the layers changed. The upper layer was the organic phase showing blue color consisting Au-thiol ligand after citrate capping was replaced by long carbon chained thiol group ($-C_{18}$) and the plasmon changed from wine red to blue. The two layers were poured down in a separatory funnel in order to recover the different layers. It was given few minutes to settle down maintaining separate layers and in the meantime, the cap of the separatory flask was kept closed as hexane is volatile. The aqueous part on the bottom part was collected back in the vial and mixed with 1 gm 1-octadecanethiol and 15 ml hexane. The vial was placed on the stirring plate again to promote more replacement of citrate capping by thiol group for next 20 minutes ensuring good mixing. The organic phase containing Au-thiol left in the separatory funnel was collected in falcon tubes (without any aqueous part as droplets). After 20 minutes, the same separating steps were followed as before to collect organic layer in falcon tubes and this time, the aqueous phase was discarded in designated place. Then, all the 6 falcon tubes with organic phase (consisting Au-thiol) were measured approximately of equal weight by adding acetone in order to make tubes eligible for centrifugation and sonicated before placing in the centrifuge. 3 cycles for 15 minutes each were operated to remove unused 1-octadecanethiol and purify Au-thiol NPs for further storage. First 2 cycles at 11000 rpm for 15 minutes each and last cycle at 9000 rpm for 15 minutes were carried on. After disposing remaining acetone from tubes, the Au-thiol NPs attached on the falcon tube's wall was dispersed in final dispersion medium chloroform and sonicated before storing in a glass bottle. The glass bottle was wrapped with aluminium foil to avoid direct light interference and kept in the refrigerator.

3.3. Deposition of Nanoparticles:

Different deposition techniques for the case of hydrophilic Au-citrate NPs on hydrophilic PVDF and Au-thiol in hydrophobic Polypropylene ($PP_{0.2\mu m}$) were tried such as spin coating and evaporation. For the evaporation, membranes were placed on the module shown later in the report and bottom 2 parts of the modules were screwed down to prevent leakage. The lid was kept open for 2-3 days to promote evaporation. In case of spin coating, there are two stages of the rotation

speed; first stage (rpm ranging 300-1000) is relatively lower to help the solution get coated on the membrane while spinning and second stage rotation rate (rpm ranging 1000-3000) is higher which helps to evaporate excess solvent. Different volumes of Au NPs suspended solution were also experimented with to have better coverage over the whole membrane.

3.3.1. Filtration of the Au-citrate and Au-thiol on respective membranes:

The filtration unit was used to deposit the NP solution on the top of the hydrophilic and hydrophobic membrane. As the unit was connected to vacuum pump, the solvent got sucked to the bottom part and NP created a filtered cake on membrane. The small particles can go directly to the bottom part of the unit sliding through the pores of the membranes while vacuum pump is working. As Au-citrate NPs are in an aqueous suspension, using filtration unit made by plastic, it is expected to be fine to carry on the filtration. But Au-thiol NPs are dispersed in chloroform which might not be compatible with plastic filtration unit. So to be in the safe side, Au-thiol NPs filtration was done using a glass filtration unit available in the lab connected to same vacuum pump.

3.3.2. Hydrophobic nanoparticles on hydrophobic membrane:

The Au NPs synthesized following the procedure described in section 3.2 imparts the quality of hydrophobicity due to the long carbon chain ($-C_{18}$). To prepare a membrane for batch experiment in membrane distillation system under test, Au-thiol NPs dispersed in chloroform was deposited on hydrophobic carbon paper. The filtration unit chosen was made by glass as glass is compatible with the dispersion medium chloroform. The comparatively smoother side of the hydrophobic carbon paper and hydrophobic PVDF was placed on the filter medium. Vacuum pump was connected to the bottom part of the filtration unit to facilitate the deposition of the Au-thiol NPs as the suspension was poured down on the membrane from the top part of the unit. The distillate collected from the bottom was disposed in the designated place.

3.3.3. Hydrophilic nanoparticles on hydrophilic membrane:

The Au-citrate NPs synthesized following the description in section 3.1 is hydrophilic as it is well dispersed in the aqueous phase which is credited to the citrate capping (-OH) of the Au NPs. Hydrophilic PVDF membrane was selected as membrane choice and placed on the filtration unit where 10 ml Au-citrate NPs suspension was poured on it. Au-citrate NPs got deposited on the membrane surface. Then the goal was to hydrophobize this surface to hydrophobic surface by changing the nanoparticles' citrate capping to thiol ligand. To achieve that the same compounds

mentioned in section 3.2 were taken in diluted concentration; 1-octadecanethiol (98%, 7 gm) completely dissolved in hexane (96%, 55 ml). Two ways were tried out to carry out the exchange and give those NPs hydrophobicity. One way was completely submerging one-quarter part of the Au-citrate NPs deposited hydrophilic PVDF into the 25 ml of the abovementioned solution. The membrane cut-out hold by a rod-clipper was suspended in one small glass beaker with 25 ml of the solution (enough volume to dip the membrane completely). The top of the glass beaker was covered with parafilm in a way so that no hexane can escape the beaker. Mild stirring mode was engaged to facilitate the interaction and maintain the mutual contact for 1 hour. Another way was to submerge one-quarter of the membrane in the flat glass petri dish containing 10 ml solution. The petri dish covered properly by parafilm placed on a shaker overnight and following morning. The latter procedure was repeated with the whole membrane. To check the role of concentration, same concentration as mentioned in section 3.2; 1-octadecanethiol (98%, 7 gm) and hexane (96%, 29.30 ml, tuned for the change in purity) was also employed.

3.4. Batch run with membrane:

To evaluate the performance of the membrane with deposited Au-thiol NPs under the LED source, the membrane was placed in the designed place of the crafted module. The membrane surface was wetted with 5 ml distilled water to cover the whole exposed surface at one go (replicating flash) by a syringe. The visible light coming from the LED interacted with the Au-thiol NPs and with the produced heat, some portion of that available water turned into vapor. The vapor traveled through the membrane pores and condensed into water on the bottom part of the module when it got into the contact with the comparatively colder module wall. Simple black hydrophobic carbon paper and white hydrophobic PVDF membrane choice were decided on as choices for comparing the performances with.

3.5. Characterization Techniques:

3.5.1. UV-Vis*:* To characterize the synthesized Au NPs, UV-vis double beam spectrophotometer ranging wavelength 200-900 nm was used. As Au-thiol dispersed in solvent chloroform, plastic cuvette cannot be used as they are not compatible. Quartz cuvettes (quantity:2 pieces) were ordered from Teknokroma Analítica. As both of the NPs suspensions are of colors, it is better to be cautious that the sample in the cuvette is clean, not scratched and not too opaque otherwise the beam would not be able to pass

through. The NPs sample in respective solvent in a cuvette was mixed well and properly using plastic syringe (sucking in and out the sample from the cuvette) or ultrasound bath (sonication) to keep the NPs well dispersed in the cuvette and not settle down on the bottom.

3.5.2. DLS: For the characterization of the NPs size, Dynamic Light Scattering (DLS) [BIC Particle Sizing Software] was used. For all the experiments, at least three runs were taken, and run was discarded when the standard deviation of the runs was too high which can be a hindrance for the results to be reproducible. The cuvettes were not scratched, clean. The sample were supposedly not aggregated or precipitated as the sonication procedure was done and the color was quite transparent (supporting dilution). Finally, to get rid of the bubbles before introducing in the equipment, the cuvette was tapped with finger or against the table. Count rate (preferably higher than 400 kcps), baseline index (preferably near 10), correlation factor near base line, polydispersity were kept a track of.

3.5.3. TEM: The sample grids for SEM and TEM session were prepared in the sample preparation laboratory, INA, UNIZAR.

3.6. Materials and Equipment:

3.6.1. Equipment and instrument: SEM (FEG INSPECT 50), TEM (FEI Tecnai T20), a particle size analyzer- DLS (90◦ fixed angle) at room temperature (Zeta Plus, Brookhaven Instruments Corporation, NY) was used for the characterization. UV–vis spectra were obtained on a UV–vis double beam spectrophotometer Jasco V-670 from wavelength 200-900 nm. Centrifuge Thermo Scientific HERAEUS Megafuge 16R (used in range 900-1100 rpm), TESTO 925 as thermometer to measure the temperature using K-type thermocouple, Balance PRACTUM1102-1S (capacity: 1100 g x 0.01 g and reproducibility: ± 0.01 g), LEDs (1 amp; white, UV-365 nm etc. at 95% intensity) with ISO-TECH (IPS 2010) power supply, for vapor distillation setup and for filtration STUART-RE3022C (ultimate vacuum 12 mbar abs.) were used.

3.6.2. Membrane and material: Both Durapore hydrophilic and hydrophobic PVDF membranes (filters) were ordered from Sigma-Aldrich; pore size 0.1 µm, thickness approximately 90 µm, 47 mm dia, surface plain and white, maximum operating temperature 85 ºC. It was not stated if the membranes went through any surface

modification. As an alternative option to Carbon black nanoparticles and have a fixed basis to the behavior of nanoparticles synthesized, H2315 C2/H23 C2 Gas diffusion layers (Carbon Paper); size A4, 21×30 cm, no hydrophobic treatment, thickness 250 µm was used. The raw materials needed for synthesis of Au-citrate and Au-thiol were provided by laboratory group NFP, INA, UNIZAR. All the compounds were available in the working lab and when finished, 1-octadecathiol and n-hexane were ordered from Sigma-Aldrich and Fisher scientific following necessary steps.

3.6.3. Module: Quite similar as previous semester report though there would be some changes. The same material as before was used again but the height and the arrangement of the module parts were changed due to the need of lower distance between installed membrane in the module and solar simulator (here, LED was used). Polyoxymethylene (POM), known as Delrin; crystalline structure was used for the module's body. It has a high melting point (~175º). It is considerably chemically inert, has lower water absorption and mechanical stability as well. The thermal conductivity is 0.4 $Wm^{-1}K^{-1}$ which shows that it would be good for thermal insulation with the surrounding environment as the less amount of heat loss to surrounding is expected. 1/16" plastic pipes were used for the connection. Connectors (as well as ferrule) were both plastics and stainless steel though the screws that tighten down the three parts together is made out of stainless steel.

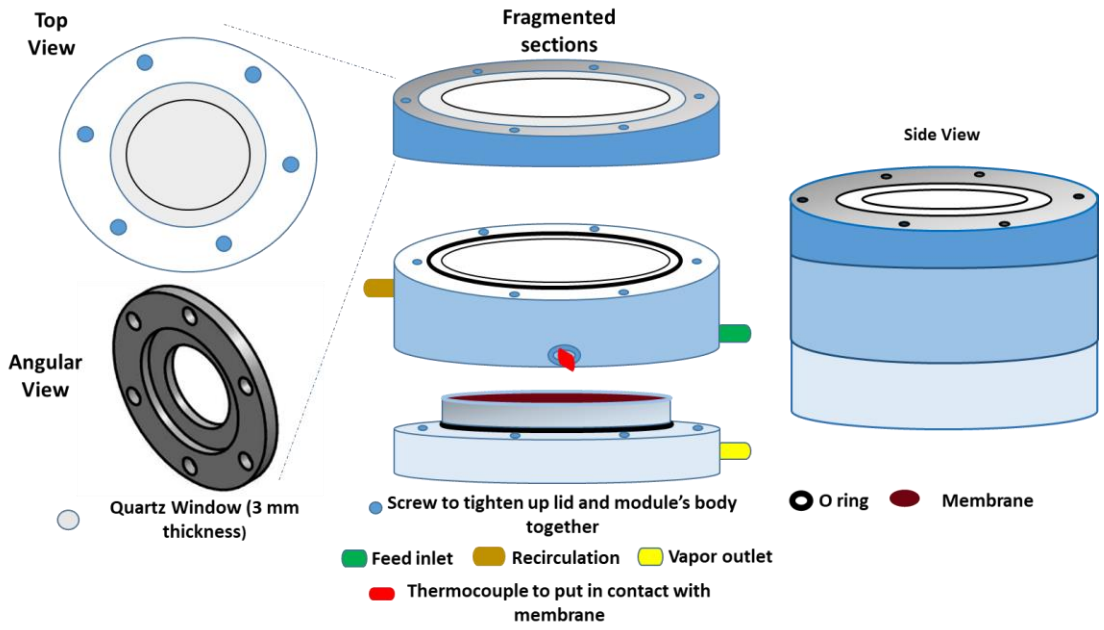

Figure 2: Membrane module and separate parts of the module (the feed entrance, vapor outlet and thermocouple ports are not shown)

In to concentrate sunlight on the membrane surface, Fresnel lens can be used which increases the irradiance up to factor of 25.[7] Here, in Figure 2, quartz window is used for focusing the light coming from LED and the thickness from the lid was cut down as much as possible keeping the necessary height to hold the window in place (resin was used to glue the window around the designed cavity). Following the expertise of the craftsman of this module, the module was built in 3 different parts as he suggested it would be easier to put the membrane in place and O-rings were placed in certain places to give it proper sealing against leaking. The thermocouple port was placed as close as membrane so that the tip of the thermocouple could touch the surface of the membrane and temperature would get registered properly when sunlight simulation would be employed with LED.

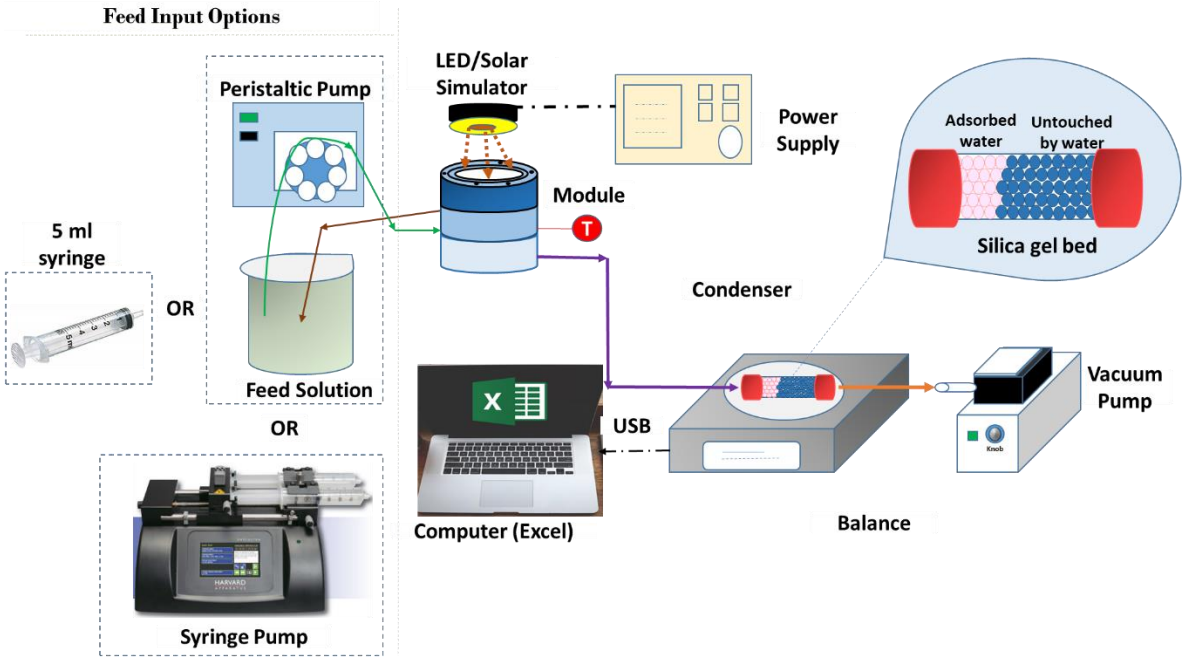

Figure 3: Nanophotonics solar membrane distillation assisted by vacuum pump (connections and order)

In Figure 3, the module is shown in complete connected system. The module was first built on thinking about using peristaltic pump and as the inlet flow rate would be a higher than the evaporated water, a recirculation connection was added to the system. Instead of peristaltic pump, syringe pump can be used as well (one or two syringes). As now for the batch experiment, 5 ml water taken by the help of plastic syringe flashed at one go on the top of membrane already placed in the module to cover the whole surface. A simple run was done to measure the least amount of water needed to cover the hydrophobic membrane surface (sample: carbon paper) and it rounded up to 5 ml. LED is used to simulate the sunlight in this system as previous semester, solar simulator was used but obtained temperature was quite low because of the lamp and membrane distance. In the previous semester, a model similar to condenser inserted into insulated flask having ice around it inside was placed on the balance to keep track of the condensate vapor. It was quite heavy altogether to be on the balance so to make it little better, it was replaced by silica bed. The balance connected to the laptop through a USB can register the weight change in excel when needed.

3.7. System Setup: Previous setup and the changes:

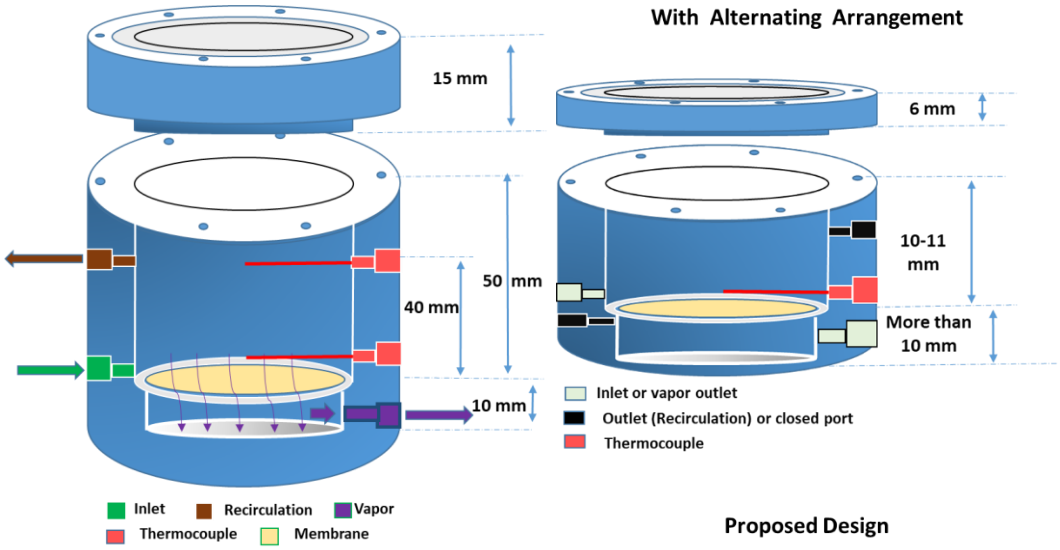

Figure 4: (left) The dimensions of the first module made; (right); the proposal of 2nd module design

The previous module (the first module built inspired by [9])with designated height is shown above in Figure 4 (left) and it is evident that only from the module, approximately 65 mm is taken into account. While experimenting, the LED should always have a certain height placed over the quartz window so that the dome and the hexagonal part of the LED do not get broken. So, other than the height of the module itself, few more mm height is added due to LED holder. Altogether, the irradiance that was reaching the membrane surface was quite low than 1 sun unit (supposedly 1 kWm^{-2}) because of this distance. So, another module design was suggested with lower height possible to get as near as possible to 1 sun unit irradiance. Due to technical obligation and suggestion from the craftsman, second version of the module was built though it was taller than the calculated value needed for possible close proximity of 1 sun unit. The dimensions of the second version of the module are added in the appendix. Though it was expected to be as low as possible in height, certain height was given to accommodate the inlet and outlet ports.

When second module design shown in Figure 4 (right) was proposed, it was made keeping in mind that this could be used for alternating arrangements meaning both hydrophilic and hydrophobic membranes. For hydrophilic membrane, the water or saline solution would be on the bottom part and for hydrophobic part as used, the water would be on the top part where vapor would make its way through the membrane to the bottom. That is why two ports are shown in the bottom side of the module in the figure.

4. Result and Discussion:

4.1. Characterization of the Au-citrate NPs and Au-thiol NPs:

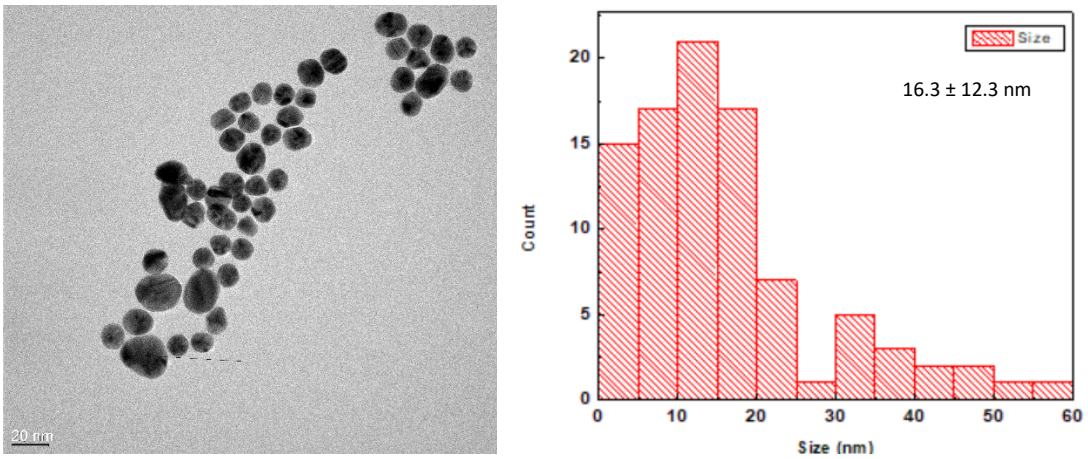

Figure 5: Au citrate nanoparticles: (left) TEM images (20 nm scale); (right) Particle size distribution from TEM images

Following the procedure described in section 3.1, Au-citrate NPs were synthesized. To characterize the NPs, they were subjected to TEM and the result is presented above in the Figure 5. Paricle size distribution shows quite a range of NPs size but maximum number of NPs are in range of 16.3 ± 12.3 nm (Count: 92). Theoratically, there would a thin layer of citrate around the Au NPs but it was quite difficult to point it out even in the highest magnification.

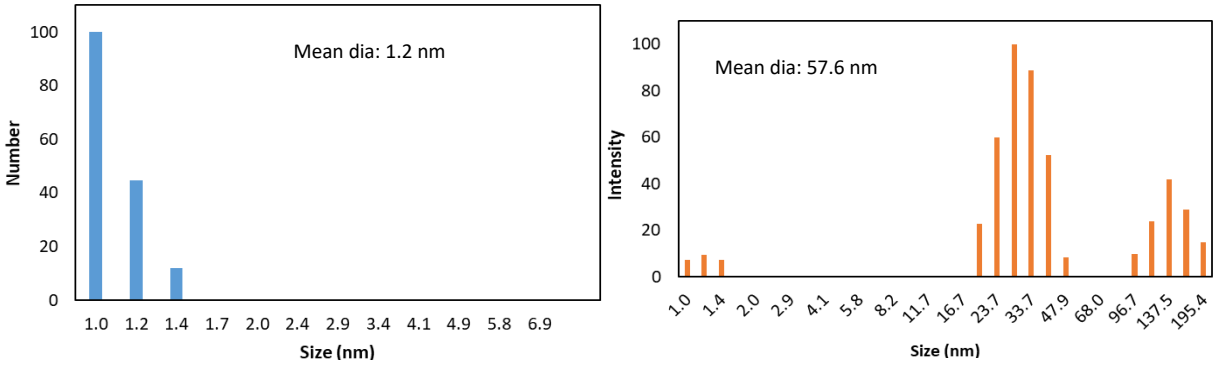

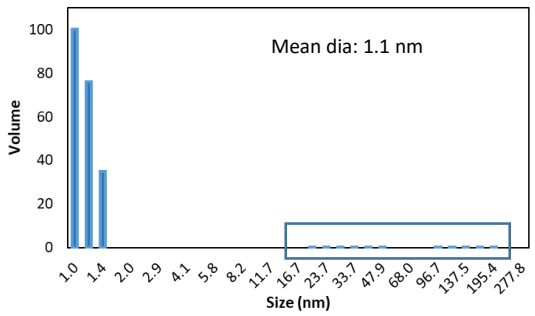

Figure 6: Particle size distribution of Au-citrate from DLS:(upper left) Number vs Size; (upper right) Intensity vs Size; (bottom) Volume vs Size

To see if the results coincide or not, it was again subjected to DLS maintaining the points stated in section 3.5 [Polydispersity: 0.23 (very high polydisperity); Count rate: 451.2; Baseline Index 9.0(7.1-10); Dust-Filter: ON]. It showed completely different results in Figure 6 which cannot be relied on. The intensity vs size graph shows it was observed that the particle sizes are apparently picked three group size; comparatively small group ranging 1-1.4 nm (approx.), middle group in 18-50 nm (approx. range) and bigger group ranging 97-160 nm approximately (agglomerates). From Figure 6, it can be misled that there are more numbers of bigger sized crystal which is not apparent in TEM particle size distribution. But in volume vs size graph, there is a hind that there could be bigger sized particles but they are really in a small amount. It could be a reason of having excess citrate in the synthesis process and the Au-citrate NPs synthesis was not centrifuged or purified. As the particle size is big, the light scattering is more intense (as the intensity is proportional to diameter,d^6) than smaller sized ones.[16] Though sonication was done to avoid aggregation and precipitation, if those are still present in the sample cuvette, it would show wrong size distribution.[17] As the Au-citrate suspension has red wine color, it is quite difficult to maintain both points- having higher count rates but not letting the cuvette sample to be opaque. If the sample is becomes too concentrated, particle sizing could be wrong multiple scattering or viscosity effects. Wrong pH, not enough sonication, not enough dilution time etc. can be an added factor to misleading particle sizing.[17]

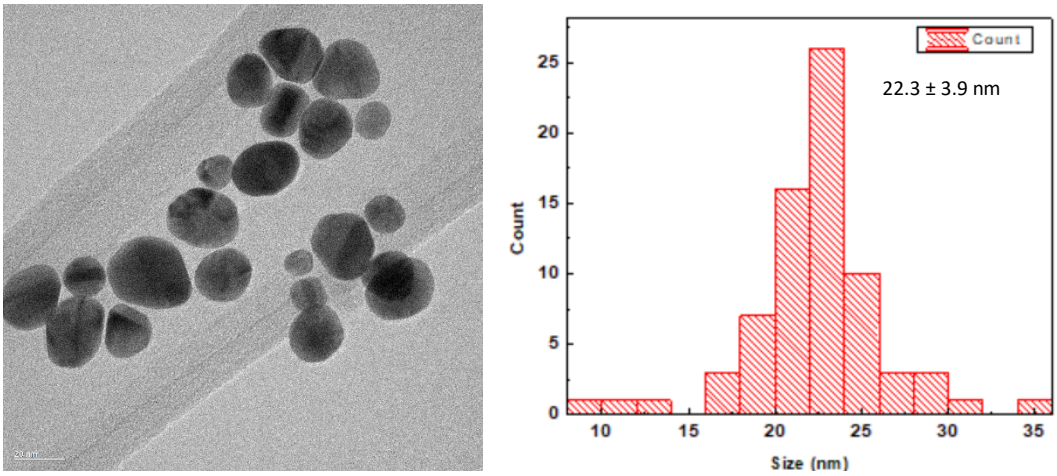

Figure 7: Au-thiol nanoparticles: (left) TEM images (20 nm scale); (right) Particle size distribution from TEM images

In case of Au-thiol NPs characterization, same characterization techniques were employed. In Figure 7, TEM images can be seen and the particle size distribution also shows that the maximum number of particles are in 22.3 ± 3.9 nm range (count: 73). The size distribution of Au-citrate and Au-thiol from TEM suggests that Au-thiol NPs are slightly bigger in size than Au citrate.

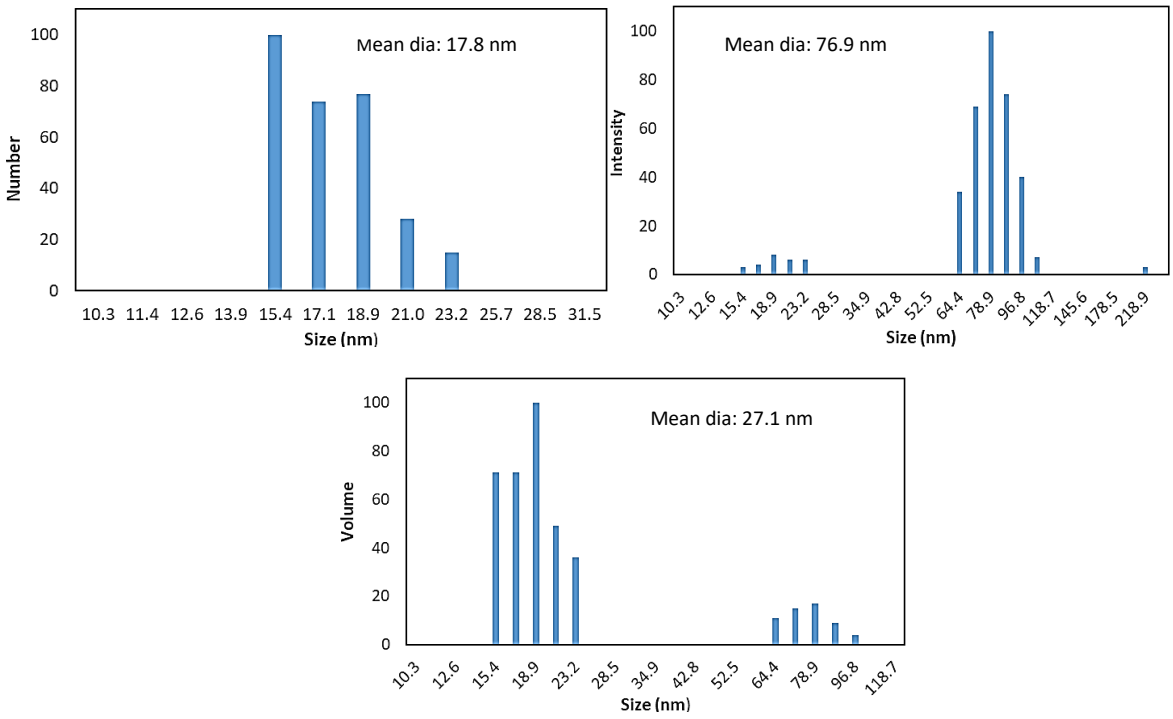

Figure 8: Particle size distribution of Au-thiol from DLS:(upper left) Number vs Size; (upper right) Intensity vs Size; (bottom) Volume vs Size

In Figure 8, the size distribution for the Au-thiol in DLS is presented [Polydispersity: 0.193 (high polydispersity); Count rate: 441.8; Baseline index: 9.4; Dust Filter: ON]. The same reasoning given for the intensity vs size graph for Au-citrate before holds ground for intensity vs size graph for Au-thiol. Bigger particles having bigger peaks do not imply that there are more large sized particles in the suspension. The number vs size (17.8 nm) and volume vs size (27.1 nm) is quite in agreement with TEM size distribution. Storing way beyond the shelf life of the NPs synthesis may also end up giving wring particle size distribution. Au-citrate dispersed in water and Au-thiol dispersed in chloroform have high shelf life (approx. 5 months).

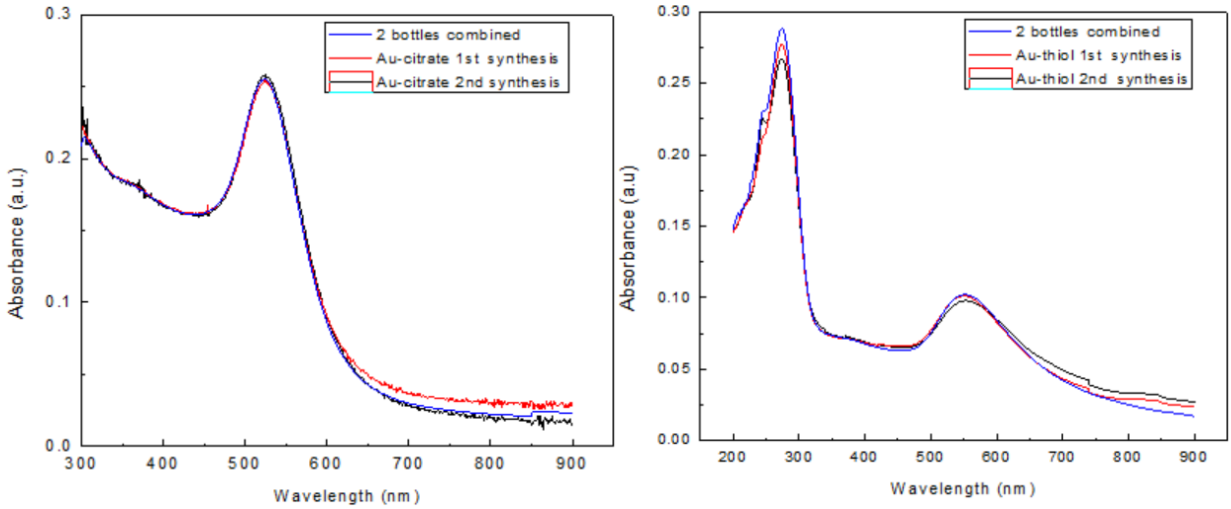

Figure 9: UV-Vis spectra for: (left) Au-citrate synthesis; (right) Au-thiol synthesis

The absorbance spectra for Au-citrate and Au-thiol are shown in Figure 9. The Au-citrate shows absorbance peak at around 530 nm and Au-thiol gives peak at approximately 560 nm. The Au-citrate peak is in agreement with other published work and it also supports the particle size found from TEM. [15][18][19][20] The Au-thiol shows two peaks- at 560 nm showing its gold part and at 280 nm (approx.) is attributed to –SH part and also the long carbon chain 1-octadecanethiol. n—σ electron transition of octadecanethiol promotes this peak around 280 (though the peak was reported at 227[21] but this paper can support the peak it states the peak shape of 1-octadecanethiol is always similar like this). Electronic transitions between the bonding and antibonding π orbital; in 180–260 nm range, the π –π* transitions appear in all the carbon materials.[22] Reproducibility of both Au-citrate and Au-thiol synthesis was good (almost same peak).

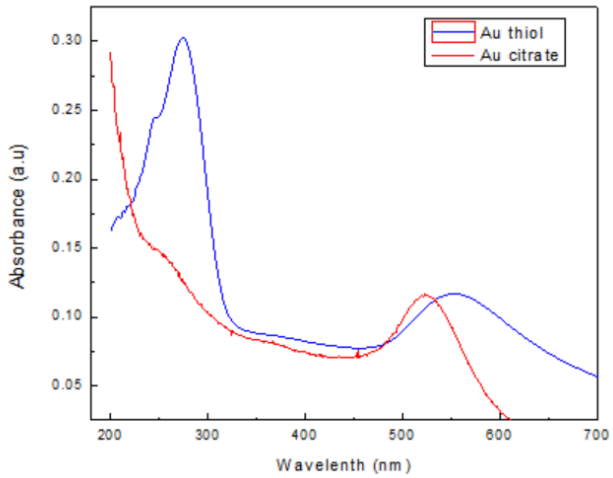

Figure 10: Comparison between the UV-Vis spectra: Red Shift of Au-thiol

In Figure 10, the comparison between Au-citrate and Au-thiol has been shown and it is evident that Au-thiol red shifted from Au-citrate moving more towards infrared area which is corresponded by the Au-S bond.[21] Also the size of the Au-thiol is slightly bigger than Au-citrate that also supports the red shift as absorption peak depends on size and shape[19][20]. So, it can be said the size difference of those two types of NPs also has an effect on the position of the peak.

4.2. Deposition of the Au-citrate and Au-thiol on the membrane:

As the synthesis process already described in section 3.1 and 3.2, it is understandable that Au-citrate is hydrophilic attributed to the –OH functional group on the other layer (dispersed media: water) and Au-citrate went through a complete conversion by replacing citrate capping with thiol chain. The chemisorption of thiols on gold is considered on the most prominent one as gold does not form a surface oxide unlike silver.[23] The sulfur from sulfydryl (SH) functional group creates a strong and robust covalent bonding with Au surface by forming gold thiolate bonding. As the thiolate–gold (RS–Au) bond strength is quite close to Au-Au bond strength, modification of Au bonding is possible for –SH group and this bonding is enough to keep the chain connected to the surface.[23][24] As the sulfur is bonded with the gold surface, the remaining alkyl chain (in this case $–C_{18}$ chain) plays role as hydrophobic part using steric hindrance. [23] This is why Au-thiol can be dispersed in chloroform but not in water.

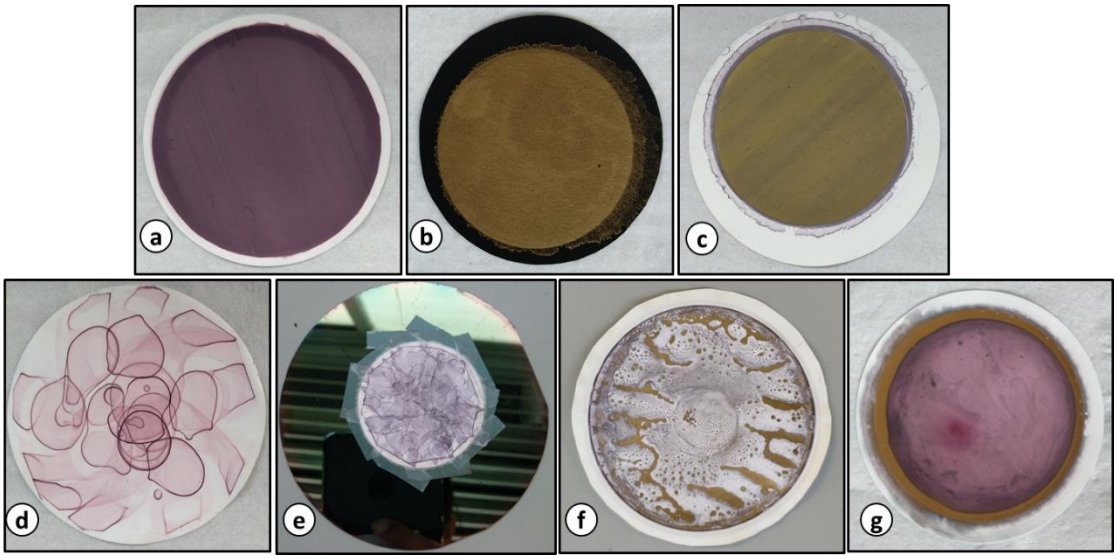

Figure 11: Filtration-(a) Au-citrate on hydrophilic PVDF; (b) Au-thiol on Carbon paper; (c) Au-thiol on Hydrophobic PVDF; Spin coating- (d) Au citrate on hydrophilic PVDF; (e) Au thiol on hydrophobic PP; Evaporation-(f) Au-thiol on PP; (g) Au-citrate on hydrophilic PVDF

Figure 11 shows different nanoparticle suspensions deposited on different types of membrane with variable deposition technique; the caption names all the nanoparticles and membranes. Evident from the figure, the acceptable coverage was obtained by filtration and that is why, filtration technique was chosen as a way of depositing NPs on membrane. Though as mentioned before, because of the different chemical behavior, the filtration takes place in plastic and glass filtration unit for respective ones.

If the Figure 11 (a) and (c) is examined closely, there are some lines evident from far also and the surface of PVDF (irrespective of hydrophilic and hydrophobic) is quite smooth whereas (b) Au-thiol on carbon paper does not show any evident lines and the deposition is quite random and dense seen by naked eyes. It can be attributed the roughness of the carbon paper. It was observed that though the suspension color was of the Au-thiol NPs was showing blue color, as soon as the suspension was deposited on the hydrophobic carbon paper, it turned golden yellowish which resembles the color quite similar to the original color of the chloroauric acid ($HAuCl_4$). The real reason behind that has to be examined. Unfortunately, any apparent reason was not found.

4.3. Electrospun embrane characterization:

The membrane preparation and production of electrospun membrane in the electrospinning were carried out following a journal paper.[25] Even thermal post-treatment (putting in the oven

overnight pressed in between glass plates) of the PVDF electrospun nanofibrous membrane was done to ensure the mechanical integrity and less membrane pore wetting.

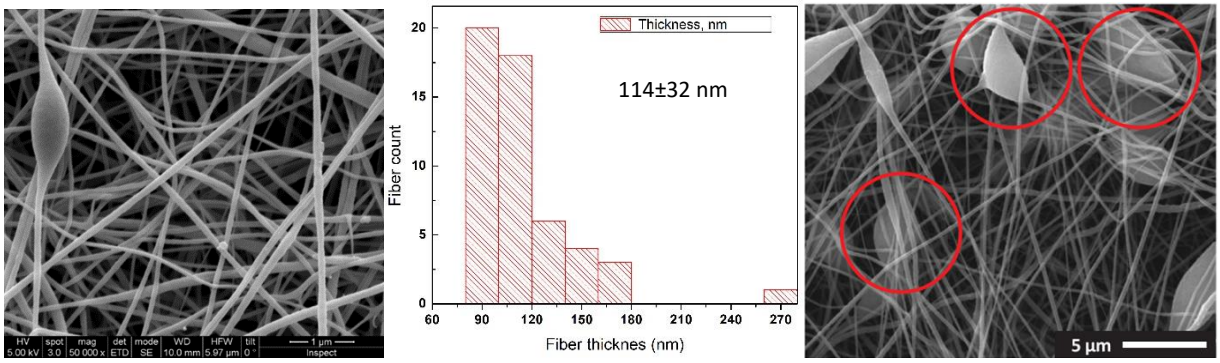

Figure 12: (left) 10 wt% PVDF Electrospum membrane SEM image of the fibers; (middle) Fiber thickness distribution; (right) electrospun membrane from paper [25]

It is reported in the journal paper that the fiber diameter of PVDF ENM 10 wt% PVDF/ $Ru(phen)_3$/LiCl ENM 145 ± 12 nm (not particularly about 10 wt% PVDF+ LiCl).[25] But in our case, the fibers' diameter is quite diverse and dispersed compared to the journal. The majority of the fiber diameter resided in the range of 114 ± 33 nm and also the non-uniformity of the fibers can also be observed in the right side photo. The electrospun membrane thickness (10 wt%) [5 hrs] was 25 ± 2 (reportedly up to 50 µm for 10 wt%) and (8.86 wt%) [8 hrs] was 55 ± 3 whereas commercial PVDF membrane thickness varies in range: 80-140 µm. As journal paper mentions the advantages of electrospun membrane, this option was also tried to have a variation in the membrane types.

4.4. Membrane characterization:

While discussing the NPs deposition membrane before it was mentioned that there is a clear pattern difference between carbon paper and PVDF. As the deposition technique is same, the only difference can be created because of the pattern and roughness of the mentioned membranes. Roughness quantity was not found for neither of these pattern but by physical examination, carbon paper seems way rougher than PVDF membrane. This attributes also to the contact angle measurements. Unfortunately, the contact angle was not taken by any equipment; it was done manually. So, it is quite possible that the value of the contact angles can be different.

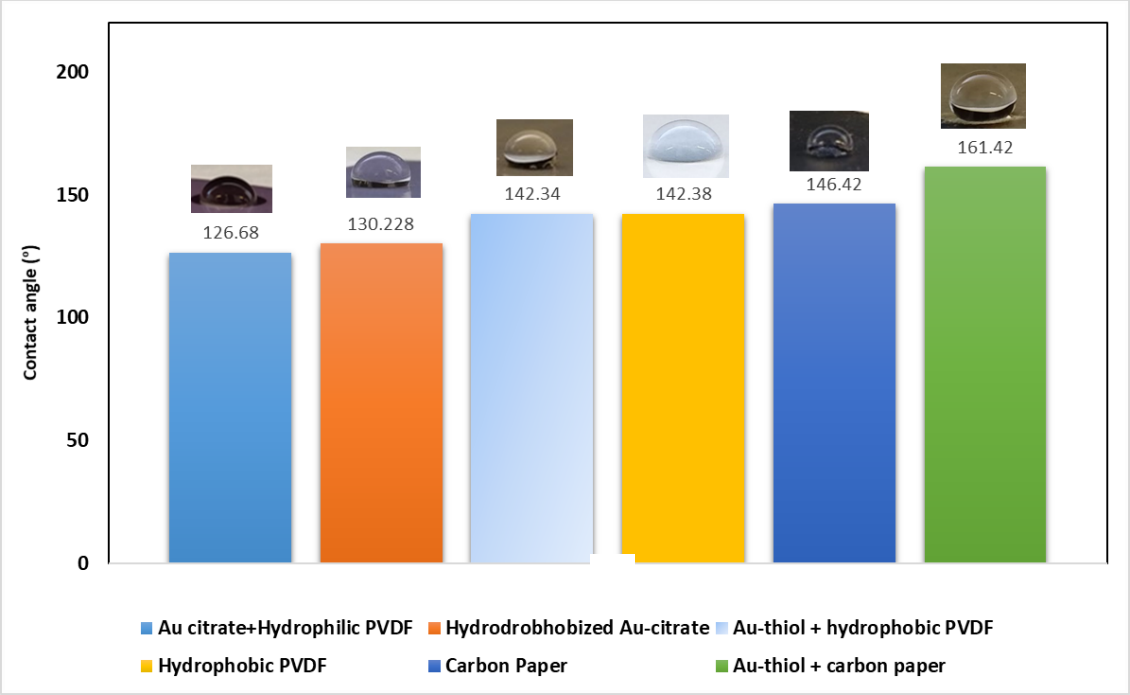

Figure 13: Contact angles for different membranes and nanoparticle deposited membranes

The drop size is also different (dropped using plastic dropper; assuming approximately 10 µl) as it was done manually. The images are treated with Imagej program with drop analysis-LB-ADSA. The measurement was not that precise to have an error bar. Just to show the comparison, the approximate and close contact angle is registered. As shown in Figure 13, the lowest contact angle is shown by Au-citrate on hydrophilic PVDF and it is understandable as the membrane itself is hydrophilic. Though normally metal imparts some hydrophobicity, it was not enough for making the hole membrane completely hydrophobic and it also might add to it that the deposition of Au-citrate was not of enough quantity to create another complete hydrophobic layer. The water still seeped through the pores quite easily and zero-time water drop gives this higher contact angle than the original membrane. As expected, when the Au-citrate on hydrophilic PVDF was exchanged to thiol ligand, it showed higher hydrophobicity and it can hold water droplet a little more than the normal Au-citrate + hydrophilic PVDF (image in Appendix). It indicates that hydrophobization of already deposited Au-citrate on hydrophilic PVDF by 1-octadecanthiol was successful to some extent but not fully successful. The Au-citrate + hydrophilic PVDF was submerged in the excess amount of 1-octadecanethiol as described in section 3.3.3 and all time contact was maintained by oscillation plate. The time and the concentration of the 1-octadecanethiol and n-hexane solution was varied but the final result did not vary that much.

The other results are quite expected as the membranes are hydrophobic membrane but the exciting result was the creation of even more hydrophobic Au-thiol surface on hydrophobic PVDF and also super-hydrophobic Au-thiol on hydrophobic carbon paper. The roughness of the carbon paper promotes more hydrophobicity playing a role in increasing the apparent contact angle.[6] Also macroscopic porosity also promotes hydrophobicity. The apparent difference of the SEM image of Quintech carbon paper and commercial PVDF is shown in the Appendix. It is clear that carbon paper has nanofiber structure whereas PVDF has sponge-like structure. It was reported that the porosity of the carbon paper is approximately 80%[26] and PVDF has approximately 70% porosity supporting the higher hydrophobicity.

4.5. Temperature profile under visible light:

Temperature measurement setup under white LED is shown in the appendix. In all temperature profile figures, if a certain time is written then it means that the certain temperature was taken for that duration. And if nothing is written that means the temperature was taken for 1:45 minute. The time duration is color co-ordinated with related trend line. No further characterization technique was not applied to see how much Sulphur (with $–C_{18}$ chain) covered the surface of the membrane when hydrophobization was carried out. It was mentioned before that sulfur and carbon chain shows absorption peak at lower 300 nm wavelength which is not covered by the acting White LED wavelength. So, it is assumed that the temperature profile of hydrophobized Au-citrate and hydrophilic membrane would be quite similar to only Au-citrate and hydrophilic PVDF.

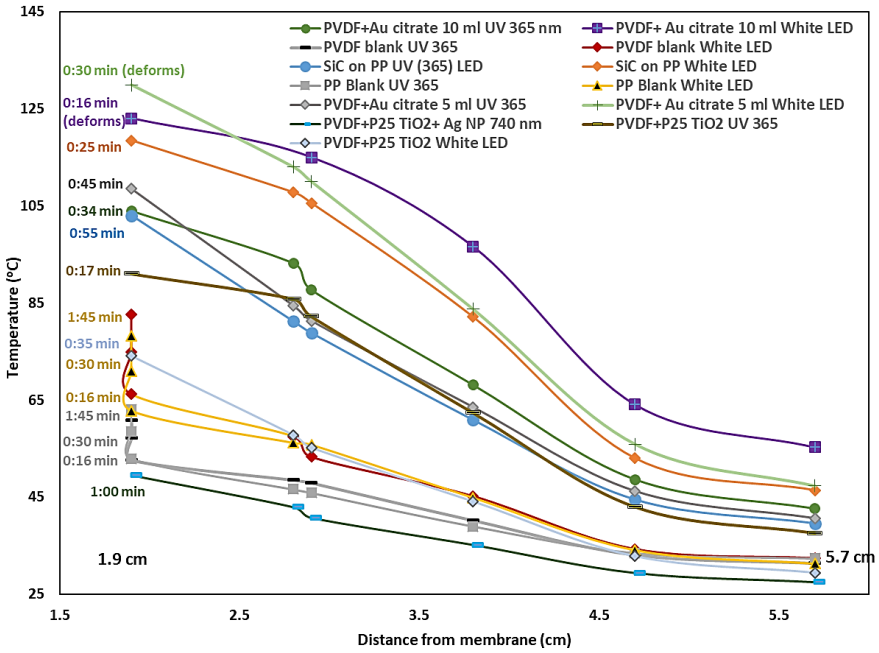

Figure 14: Temperature Profile for various combination of membranes and nanoparticles using UV 365 nm LED, White LED, 740 nm wavelength LED: Temperature vs distance of the LED source from the membrane (lowest and highest distance 1.9 and 5.7 cm respectively)

More to this point, batch experiment was run on the hydrophobized membrane but it was not enough hydrophobic to hold up the water at top of it. Really soon, after the experiment started assisted by vacuum pump, all the went to the bottom part. That is why, the temperature profile and results of the batch experiment of hydrophobized Au-citrate + hydrophilic PVDF will not be shown and discussed. Figure 14 shows the temperature profile of blank membranes and also that of incorporated different NPs option on the available membranes. Expected result was obtained when the experiments of the blank membranes $PVDF_{0.1\mu m}$ and Polypropylene ($PP_{0.2\ \mu m}$) showed that the temperature rise was quite low compared to the membranes with NPs. Au-citrate NPs, commercial SiC, triangular shaped Ag NPs were taken into account. Latent heat of vaporization for the phase change from liquid to vapor Under plasmon resonance conditions, ten times more heat flux than that of Au NPs can be produced by Ag NPs.[9] SiC (powder form) had to be dispersed in ethanol solvent and that is why hydrophobic PP membrane was chosen for that. The other NPs were deposited on hydrophilic PVDF as the solvent of those NPs were water. Again, filtration unit was used to deposit the NPs on membrane. In case of Ag NP, not much NPs stayed on the top of membrane and that is why another layer of P25 TiO_2 was deposited on PVDF before filtration of Ag NPs. As for the specific size and shape (absorption peak approximately 750 nm), it was

expected that it would excite well under available LED wavelength 740 nm but it shows the lowest temperature rise. Probable reason: a) change of triangular shape of Ag NPs; b) TiO_2 does not cover that absorption range; c) very less amount of Ag NP stayed on the top of the membrane. For these reason, this Ag NP incorporation with membrane was not produced. SiC NP though showed modest temperature rise but there used to be some loose SiC NPs on the water as SiC was loosely attached to the membrane surface. At last, Au-citrate was deposited on hydrophilic PVDF membrane which showed good coverage (red wine color quite homogeneously all over the membrane). 5 ml and 10 ml was deposited on the PVDF membrane and the latter one showed dense color supporting good coverage. The temperature profile of these two membrane was done under white LED and UV 365 nm LED option. 10 ml Au-citrate showed the highest temperature profile under white LED. This is why, this option was chosen to be continued with. Even the PVDF membrane got deformed for both Au-citrate deposited membrane as the temperature rose really high than it can handle (rose higher than 123 ℃). Au NPs photothermal efficiency was studied with femtosecond transient absorption spectroscopy which showed that when metal nanostructure gets excited under illumination (photoexcitation), it produced heated electron gas that which cools really quickly like in ∼1 ps. Nanoparticle lattice cools down fast by exchanging energy with the surrounding medium within∼100 ps (due to phonon–phonon interactions). This fast excitation and exchange of energy results heating of the local surrounding environment. It only needs light radiation with a frequency strongly overlapping with the nanoparticle surface plasmon resonance absorption band (wavelength covering the range of the adsorption peak or range).[19] Those experiments showing temperature profile helped to decide on the future work which would include Au citrate (10 ml) deposited in hydrophilic membrane. But as one of the most basic trait of Membrane distillation is membrane has to be hydrophobic, hydrophobizing this membrane was tried keeping intact its temperature profile but to improve its hydrophilicity to hydrophobicity with 1-octadecanethiol (described before).

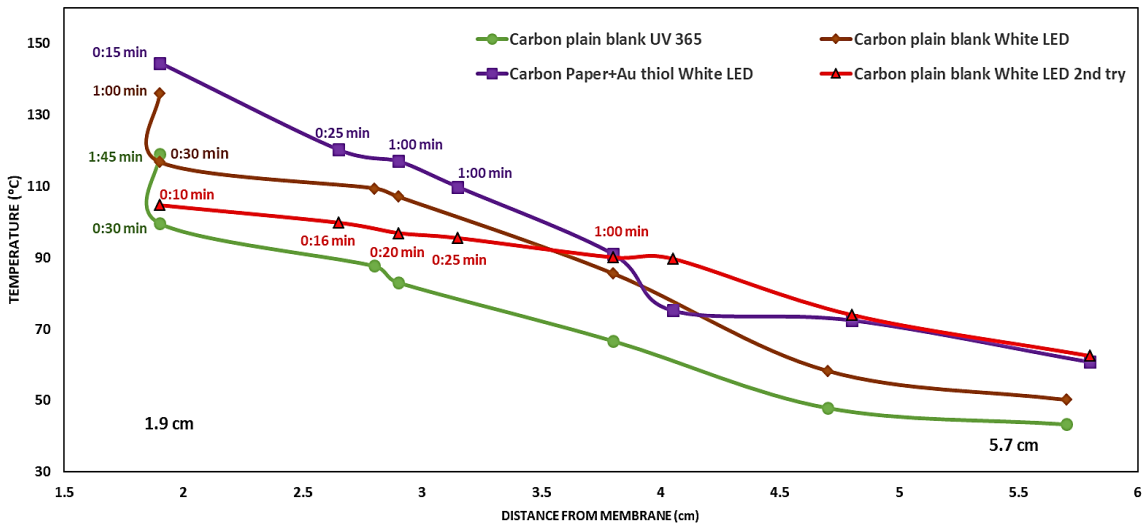

*Figure 15: Temperature profile for **Carbon Paper**: under UV 365 and White LED: Temperature vs distance of the LED source from the membrane*

As it was realized in the literature review part, much work has been done using Carbon black NPs or graphite layer. To evaluate the possibility of using gas diffusion layer (carbon paper layer) as convenient option for membrane distillation and to see where is stands on, temperature profile was taken and presented in Figure 15 (only with carbon paper). Under UV 365 LED, it showed lowest rise compared to the other options. The highest temperature was obtained the Au-thiol deposited on carbon paper under white LED. It was quite expected as both, carbon and Au-thiol would get excited by the applied illumination and would both add up to the temperature. But one inconsistency was observed as the blank experiment of temperature rising under White LED was done twice and it gave different profiles. The probable reason was thought as maybe the first try, the dome of LED had some crack and the temperature could not rise at first (as the temperature difference on the higher distance from membrane is more than 10 °C) and the temperature rose in 1:45 min for first try which on second try, reached quite quickly near that temperature (nearly 20 sec or more). That first try experiment was done with different LED connection. All the other ones have been done with same LED connection and it was checked properly that it did not have any crack. Though, further or more experiment would help to have a concreate reason to decide on which one is the right profile.

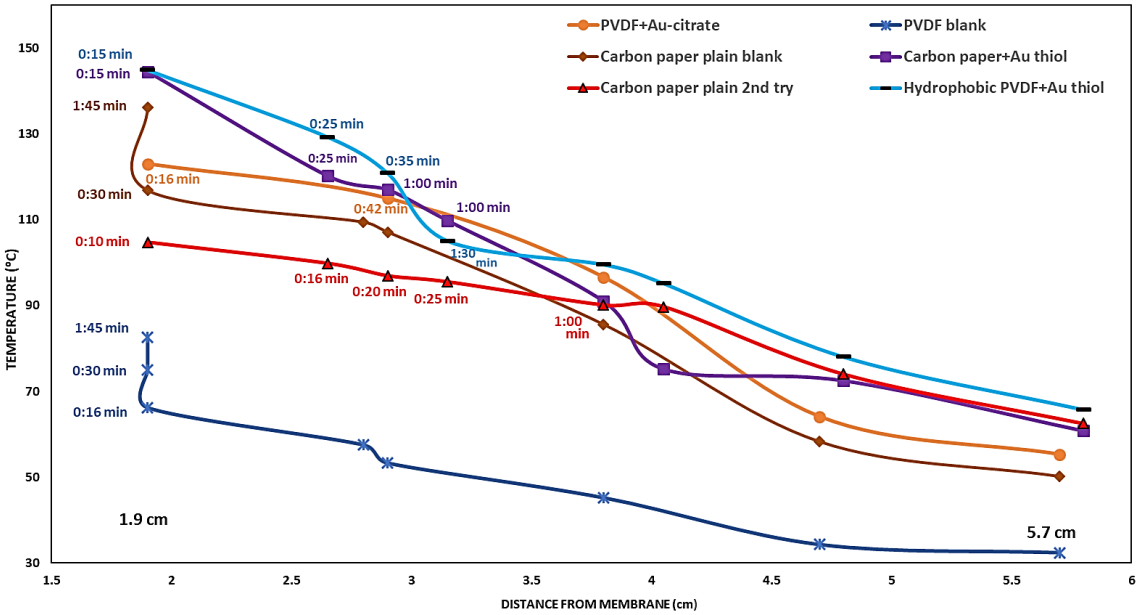

Figure 16: Temperature Profile of different membrane and nanoparticles combination under White LED: Temperature vs distance of the LED source from the membrane

Figure 16 shows the similar temperature profiles shown in Figure 13 but the difference is that those temperature profiles were overlapped with other membrane options shown in the onset. To have a basic idea how much the blank PVDF and blank carbon paper helps to rise the temperature, they were included in this graph. As Au-thiol deposited on carbon paper might work as a bilayer membrane option (6 ml Au-thiol chloroform was deposited), to compensate a little bit for blank PVDF hydrophobic membrane, 10 ml Au- thiol was deposited on the membrane. Also 10 ml volume was chosen to have a comparison with 10 ml Au-citrate solution deposited on hydrophilic membrane. One thing to clear: while filtration, some Au-citrate NPs goes along with the filtrate (has faint wine-pinkish color to it; goes through the membrane pore to bottom) but the filtrate after Au-thiol filtration does not show much color (original color darkish blue). This is only an observation by naked eye. To compare the values, further tests (concentration measurement including) should be done. Carbon paper + Au thiol and Hydrophobic PVDF+ Au thiol reached same temperature at the same time. Probable reason could be Au-thiol is taking the front sit and temperature rise is contributed mostly by Au-thiol. Au citrate gets to higher temperature than carbon paper only. A thin circle around the edges of PVDF membrane was not covered by Au-thiol when filtrated and was exposed to the White LED as blank PVDF) during the experiment. From the profile trends, it can be said at least extra Au-thiol added to blank PVDF acted quite effectively to add to temperature rise compared to carbon paper. To explain this point, a picture is

added to the appendix. Carbon paper + Au thiol and Hydrophobic PVDF + Au thiol shows quite similar tend though latter one has more fluctuation added to it (temperature taken for different time range)

The temperature profiles in terms of irradiance are included in the appendix.

4.6. Batch Experiment result:

As described before section 3.4, batch experiments were run and the results are presented in the Figure 17. The experiment was tried to do perform under same vacuum pressure (3-3.5 in Hg). This pressure chosen using carbon paper and hydrophobic PVDF as experiment basis.

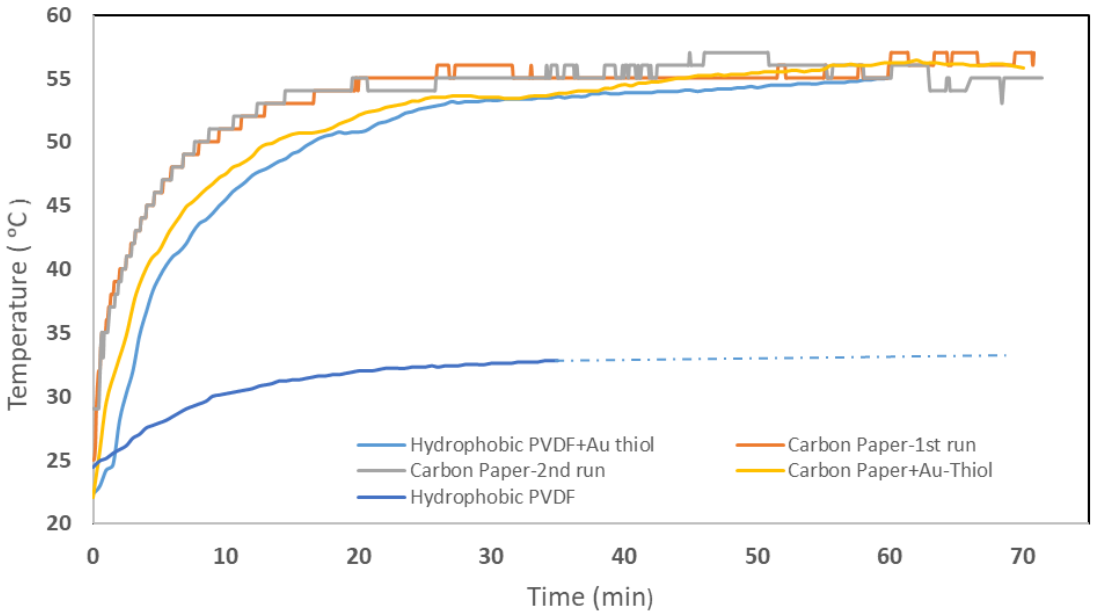

Figure 17: Batch experiment for different NPs and membrane combination

It was decided after careful tuning to choose the maximum pressure which facilitates the process but does not intervene the experiment by drawing down the allotted water on the top of the hydrophobic membrane. To check the performance of the electrospun membrane, it was also subjected to batch run. But it had a really thin thickness compared to the commercial ones. And under this vacuum pressure, it was unable to maintain its shape. It showed good hydrophobicity but due to low thickness, membrane got drawn towards bottom part taking a shape like upside hat.

From the temperature profile it was observed that Au thiol + hydrophobic PVDF has better temperature form (worked under closed air) than blank carbon paper. But in the batch experiment, the carbon paper showed better temperature profile than every other option which is not in

agreement with the previous results shown. One reason could be that the carbon paper has a head start with higher stating temperature point (approximately 29 ºC for both runs) compared to others (the other experiments started at approximately 22 ºC). The reproducibility of blank carbon paper experiment is really good as it gave quite similar trend and assumed steady state.

The hydrophobic PVDF showed its hydrophobicity and it let a very negligible amount of water from upper part to bottom side when the white LED was illuminated and placed on top of the module. Exposed membrane are in the module under LED is 11.34 cm^2 under irradiance 0.71 kWm^{-2}.

A problem was faced with the stability of the balance because of the vibration of the existing vacuum pump. While vacuum pump running, the loud vibration of that placed on the same table as the other parts of the system did not let register the weight difference in the silica gel bed. To get an approximate value of the flux, remaining water from 5 ml still remaining on the top of the membrane was collected and weighed. For pure water, the permeate flux for only carbon paper was 17.5 $gm^{-2}s^{-1}$ whereas with membrane area 21.24 cm^2 and for 15% Ag NP loading in PVDF membrane [vacuum pressure of 20 mbar (0.59 in Hg) and initial feed temperature of 303 K, irradiance 23 kWm^{-2} giving average transmembrane flux for pure water following 4.08 $gm^{-2}s^{-1}$ [9] The higher vacuum pressure might have facilitate the vapor permeation and condensation. Photothermal effect of Au NP and Ag NP also could play a deciding factor.

For Au thiol deposited on carbon paper gives 23.93 $gm^{-2}s^{-1}$. When a gas diffusion layer like the one in our experiment is compressed, the fiber to fiber contact increases and results into increase of effective thermal efficiency.[27] This might have helped to have higher temperature gain and transfer of the thermal effect for carbon paper. And also is it really hydrophobic and has higher porosity, vapor permeation though pore would have been helped.

Au thiol on hydrophobic membrane gives 21.56 $gm^{-2}s^{-1}$ permeate flux. Though the temperature profile was quite similar to the abovementioned membrane, porosity and hydrophobicity were different. And also good coverage of Au-thiol NP could have been a help to increase the flux a little better.[8] As all the calculation was done manually, a large percentage of error is also expected.

5. Conclusion:

Membrane distillation has always garnered attraction for one of the convincing and feasible ways for desalination and in today's world, looking for alternative ways to improve existing system and achieve something helpful to mankind using renewable energy is always appreciated. Among all the available membrane distillation type, nanophotonics enabled solar membrane distillation was chosen to explore in this project. To use the most out of the surface plasmon resonance of the nanoparticles maintaining all the crucial requirements intact (hydrophobicity) was one of the goal in this project. Spin coating, simple evaporation and filtration were tried to find the best one which gives the high coverage of the hydrophobic (hydrophilic as well) and filtration showed the most promising result. Different nanoparticles with different membranes made combination and relatively best one was selected keeping in mind the hydrophobicity of the membrane, temperature profile and flux. Characterization of Au-citrate and Au-thiol was done using TEM and DLS, UV-vis spectroscopy. Though carbon paper was hydrophobic at the first place, Au-thiol deposited on the carbon paper gives super-hydrophobicity which could be attributed to the roughness and fiber arrangement of the carbon paper. It also gives the highest flux rate 23.93 $gm^{-2}s^{-1}$ compared to other membrane arrangements. Exploring and testing out gas diffusion later (carbon paper) along Au-citrate and Au-thiol incorporated membranes gave new insight which may be of help in near future.

6. Future Plans:

Quartz window can be replaced by Fresnel lens in the existing module. Electrospun membrane fabricated more than 8 hours to get the desired thickness may add up another membrane option. Correct concentration measurement for the nanoparticles could be valuable to quantify the dosage or loading. The vacuum pump can be isolated from the system environment moving to other place connecting with longer connecting pipe. Another vacuum pump regulated by sustainable valve which does not weigh down the silica gel bed on the balance could be also another modification. Another way could be introduction of sweeping gas on the bottom part to take away the condensate and for that slight change in the port design in the module has to be done. Other compounds like silane compounds with varying concentration, contact time with the exchanging solution can be used to hydrophobize the hydrophilic surface other than 1-octadecanethiol. New nanoparticles can be explored as alternate option to broaden the coverage of solar spectrum (not only visible light).

Installing the existing module or improved and modified module under direct sunlight is one of the aspiring goals to reach.

7. Bibliography:

1. Gopi G, Arthanareeswaran G, Ismail AF. Chemical Engineering Research and Design Perspective of renewable desalination by using MD plant capacity. Chem Eng Res Des [Internet] 2019;144:520–37. Available from: https://doi.org/10.1016/j.cherd.2019.02.036
2. Naidu G, Geun W, Jeong S, Choi Y, Ghaffour N, Vigneswaran S. Transport phenomena and fouling in vacuum enhanced direct contact membrane distillation : Experimental and modelling. Sep Purif Technol [Internet] 2017;172:285–95. Available from: http://dx.doi.org/10.1016/j.seppur.2016.08.024
3. Saffarini R, Arafat H, Thomas R. INFLUENCE OF PORE STRUCTURE ON MEMBRANE WETTABILITY IN MEMBRANE. 2012;(March):1–5.
4. Wu J, Zodrow KR, Szemraj PB, Li Q. Photothermal nanocomposite membranes for direct solar membrane distillation. J Mater Chem A 2017;5(45):23712–9.
5. Cipollina A, Di Sparti MG, Tamburini A, Micale G. Development of a Membrane Distillation module for solar energy seawater desalination. Chem Eng Res Des [Internet] 2012;90(12):2101–21. Available from: http://dx.doi.org/10.1016/j.cherd.2012.05.021
6. Kuo C, Lin H, Tsai H. Fabrication of a high hydrophobic PVDF membrane via nonsolvent induced phase separation. DES [Internet] 2008;233(1–3):40–7. Available from: http://dx.doi.org/10.1016/j.desal.2007.09.025
7. Dongare PD, Alabastri A, Pedersen S, Zodrow KR. Nanophotonics-enabled solar membrane distillation for off-grid water purification. 2017;1–6.
8. Wu J, Zodrow KR, Szemraj PB, Li Q. Photothermal nanocomposite membranes for direct solar membrane distillation. J Mater Chem A 2017;5(45):23712–9.
9. Politano A, Argurio P, Di Profio G, Sanna V, Cupolillo A, Chakraborty S, et al. Photothermal Membrane Distillation for Seawater Desalination. Adv Mater 2017;29(2):1–6.
10. Lewis NS. Solar Energy Use. 2007;(February):798–802.
11. Neumann O, Urban AS, Day J, Lal S, Nordlander P, Halas NJ. Solar Vapor Generation Enabled by Nanoparticles. 2013;(1):42–9.
12. Ghasemi H, Ni G, Marconnet AM, Loomis J, Yerci S, Miljkovic N, et al. Solar steam generation by heat localization. Nat Commun [Internet] 2014;5:1–7. Available from: http://dx.doi.org/10.1038/ncomms5449
13. Fujiwara M, Imura T. for Water Puri fi cation and Desalination Using Azobenzene Modi fi ed Anodized. 2015;(6):5705–12.

14. Bae K, Kang G, Cho SK, Park W, Kim K, Padilla WJ. Flexible thin-film black gold membranes with ultrabroadband plasmonic nanofocusing for efficient solar vapour generation. Nat Commun [Internet] 2015;6:1–9. Available from: http://dx.doi.org/10.1038/ncomms10103

15. Lafuente M, Pellejero I, Sebastián V, Urbiztondo MA, Mallada R, Pina MP, et al. Sensors and Actuators B : Chemical Highly sensitive SERS quantification of organophosphorous chemical warfare agents : A major step towards the real time sensing in the gas phase. Sensors Actuators B Chem [Internet] 2018;267:457–66. Available from: https://doi.org/10.1016/j.snb.2018.04.058

16. Motion B. Dynamic Light Scattering : An Introduction in 30 Minutes. :1–8.

17. Farrell E, D JBP. Guide for DLS sample preparation. 1(631):1–3.

18. Huang X, Jain PK, El-sayed IH. Plasmonic photothermal therapy (PPTT) using gold nanoparticles. 2008;217–28.

19. Link S, El-sayed MA. Shape and size dependence of radiative , non-radiative and photothermal properties of gold nanocrystals. 2000;409–53.

20. Kwon K, Lee KY, Lee YW, Kim M, Heo J. Controlled Synthesis of Icosahedral Gold Nanoparticles and Their Surface-Enhanced Raman Scattering Property. 2007;1161–5.

21. Li W, Ren Y, Xu R, Ding H, Xi S. Langmuir — Blodgett films of octadecanethiol on gold sols subphase. 1998;5(98):603–5.

22. Microwave Assisted Synthesis and Characterizations of Decorated Activated Carbon. 2012;(May 2014).

23. Love JC, Estroff LA, Kriebel JK, Nuzzo RG, Whitesides GM. Self-Assembled Monolayers of Thiolates on Metals as a Form of Nanotechnology. 2005.

24. Häkkinen H. The gold–sulfur interface at the nanoscale. Nat Chem [Internet] 2012;4(6):443–55. Available from: http://dx.doi.org/10.1038/nchem.1352

25. Santoro S, Vidorreta IM, Sebastian V, Moro A, Coelhoso IM, Lima JC, et al. A non-invasive optical method for mapping temperature polarization in direct contact membrane distillation. J Memb Sci [Internet] 2017;536(April):156–66. Available from: http://dx.doi.org/10.1016/j.memsci.2017.05.001

26. Ramousse J, Didierjean S, Lottin O, Maillet D. Estimation of the effective thermal conductivity of carbon felts used as PEMFC Gas Diffusion Layers. 2008;47:1–6.

27. Bock R, Shum AD, Xiao X, Karoliussen H, Seland F, Zenyuk I V, et al. Thermal Conductivity and Compaction of GDL-MPL Interfacial Composite Material. 2018;165(7):514–25.

#Appendix:

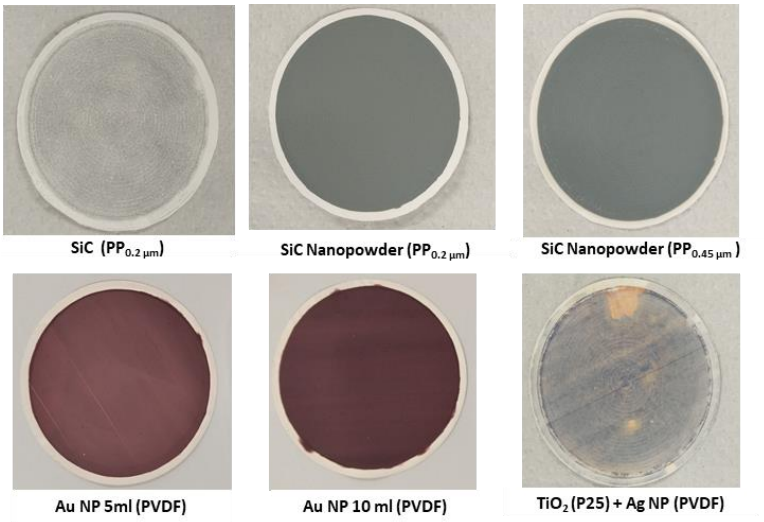

Appendix: Figure 1:Different nanoparticles filtrated on different membranes in previous semester thesis work

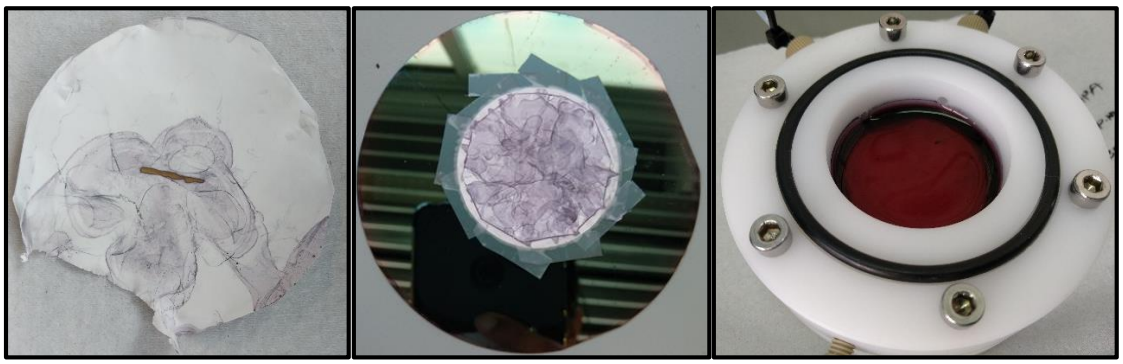

Appendix: Figure 2: (left) Breakage of PP 0.2 um membrane while spin coating of Au thiol as PP is not that compatible with chloroform; (middle) careful attachment of PP membrane on silicon wafer to avoid breakage and curling- spin coating varying spin time, spinning speed

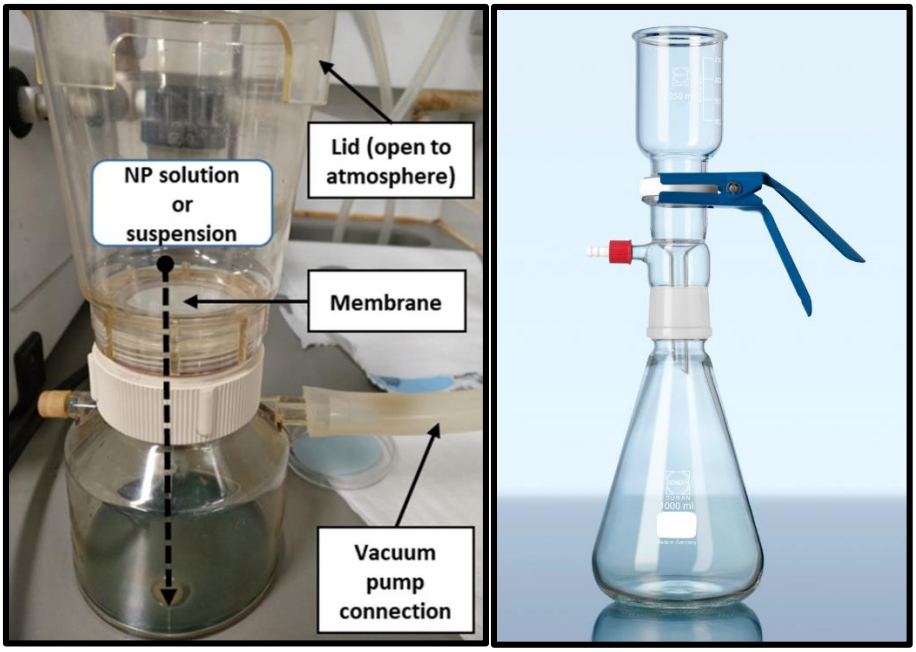

Appendix: Figure 3: Filtration unit: (left) plastic one for water and ethanol filtration ; (right) Glass filtration unit for chloroform filtration

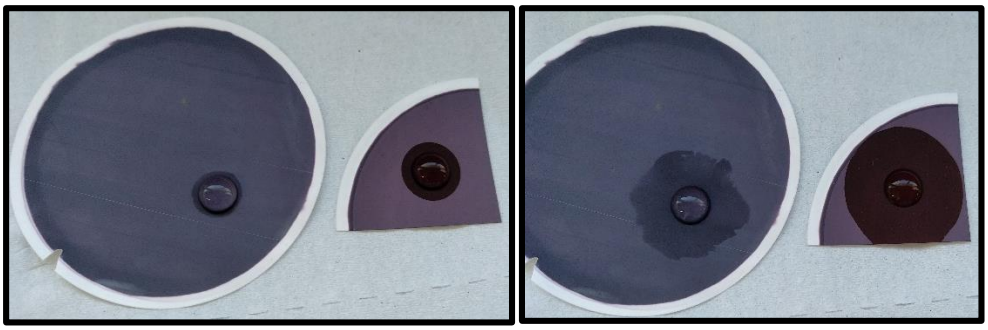

Appendix: Figure 4: Water droplet holdup by (left side of the image): Hydrophobized Au-citrate by 1-octadecanethiol; (right side of the image) Au citrate on hydrophilic PVDF [(left image):30 sec ; (right image): 3 minutes

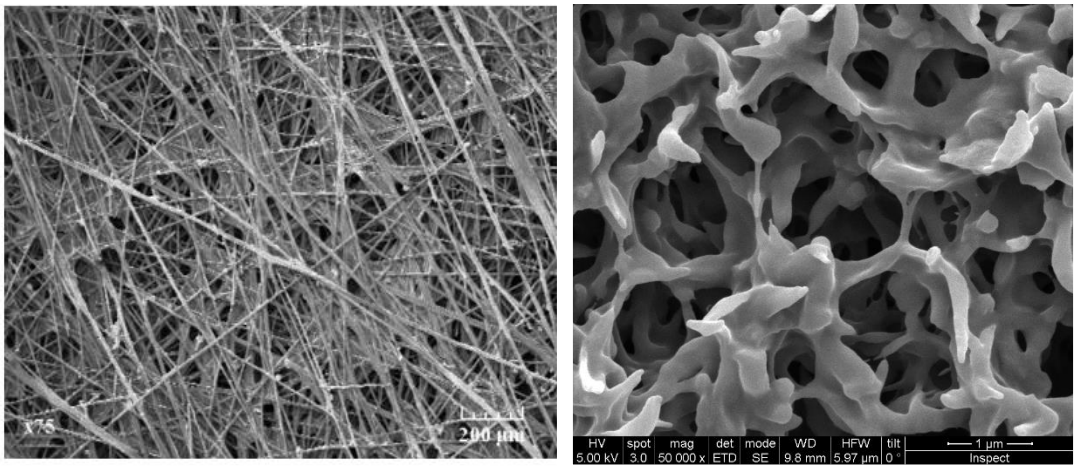

Appendix: Figure 5:SEM image: (left) Quintech Gas diffusion layer (carbon paper)[26]; (right) Spongelike PVDF membrane adds hydrophobicity [6]

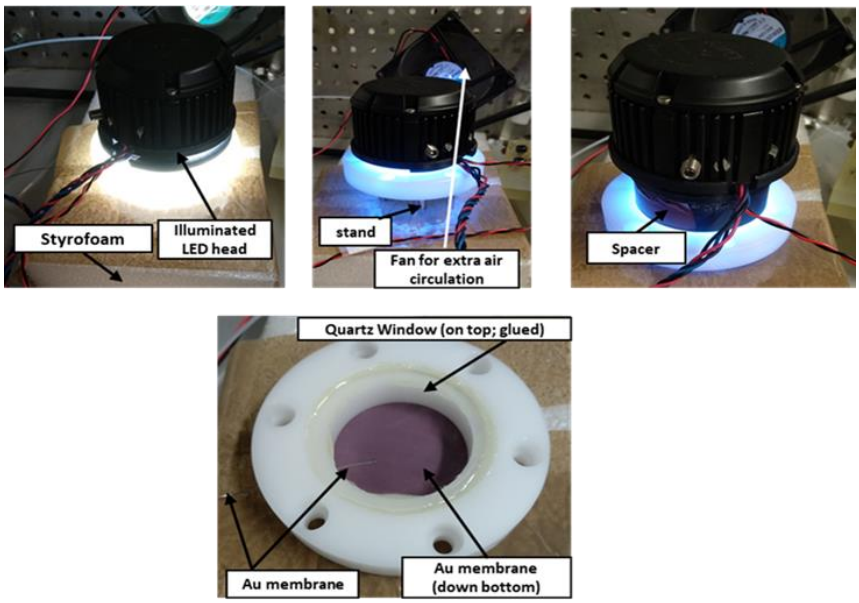

Appendix: Figure 6: System setup for measuring the temperature of NPs deposited on membrane produced by applying different LEDs of various wavelengths (the lid from first designed module; height 1.2 cm)

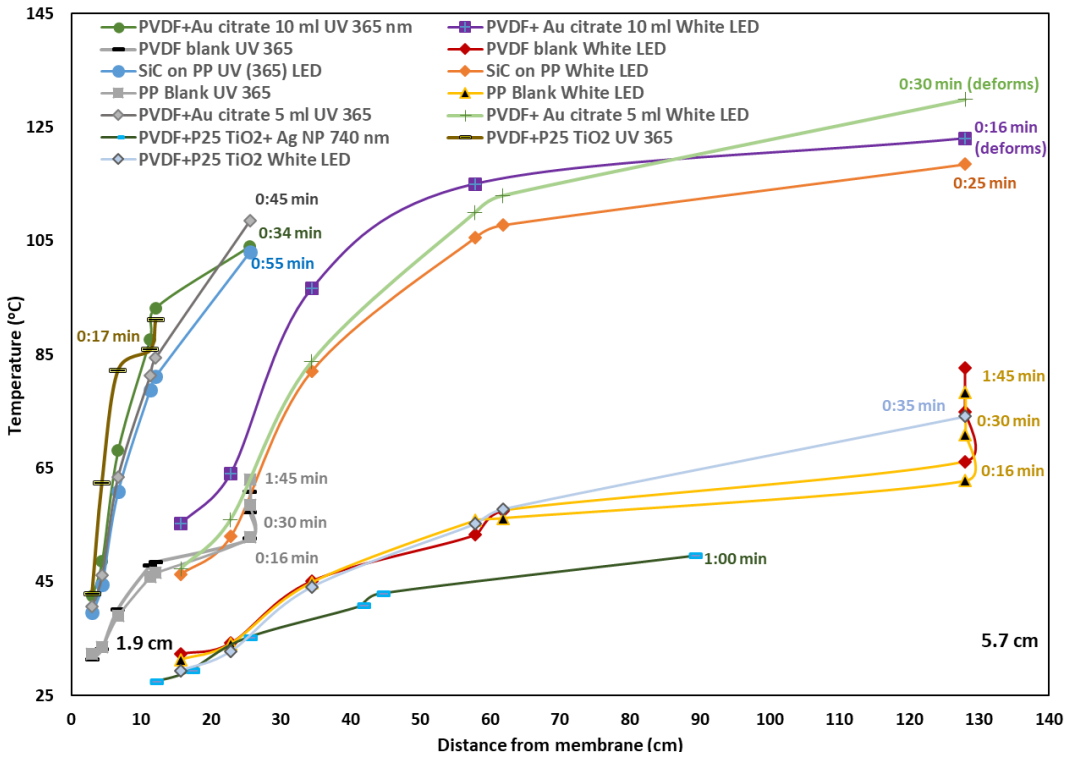

Appendix: Figure 7: Temperature profile for various combination of membranes and nanoparticles using UV 365 nm LED, White LED, 740 nm wavelength LED: Temperature vs irradiation calculated using varying distance of the LED source from the membrane

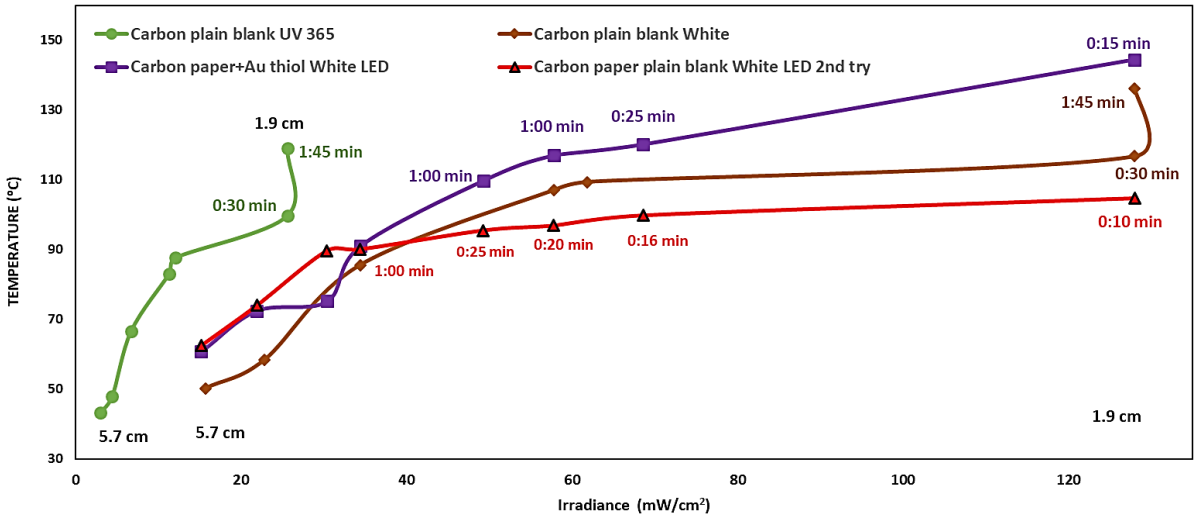

Appendix: Figure 8: Temperature profile for Carbon Paper under UV 365 and White LED: Temperature vs irradiation calculated using varying distance of the LED source from the membrane

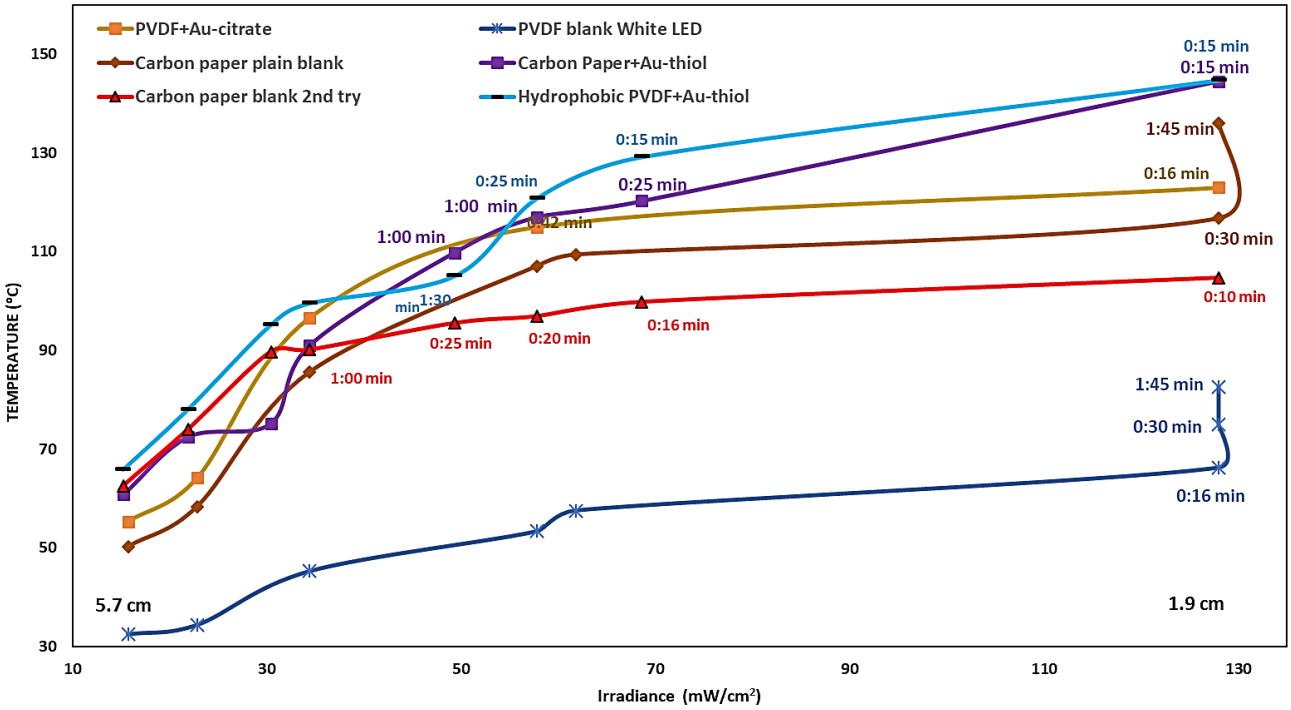

Appendix: Figure 9: Temperature profile for different membrane and nanoparticles combination under White LED: Temperature vs irradiation calculated using varying distance of the LED source from the membrane

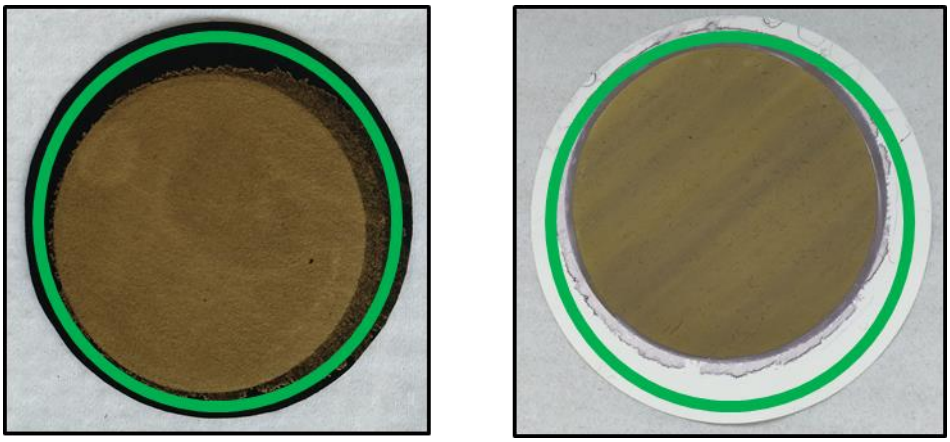

Appendix: Figure 10: The area inside the green circle still has carbon when installed to module exposed to White LED though Au-thiol does not cover the area but the same area for right image only has blank PVDF. It happened due to the smaller diameter of the filtration unit

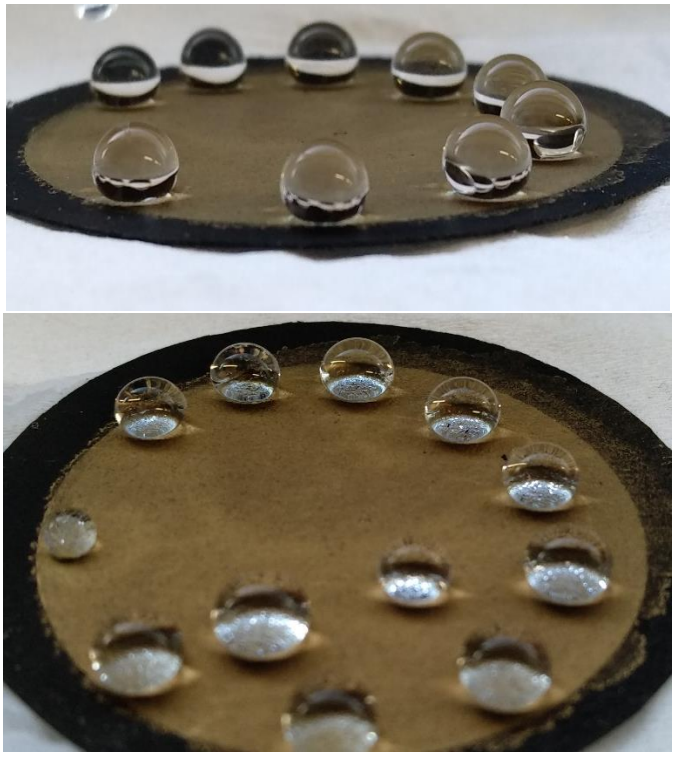

Appendix: Figure 11: Super-hydrophobic Au thiol deposited on gas diffusion layer (carbon paper)

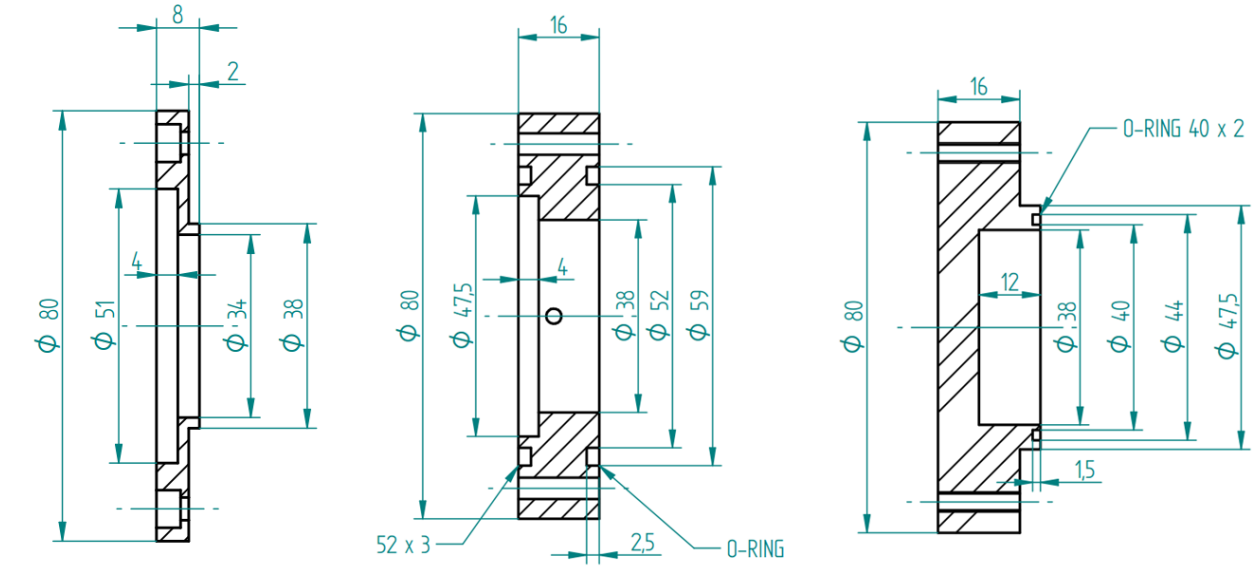

The Top or Lid with quartz window (given space 4 mm)

The middle part (exposed membrane dia 38 mm)

The bottom part (12 mm height given for vapor condensate)

Appendix: Figure 12: Dimensions of 2nd version of the module